Technical Report Documentation Page

1. Report No. FIU-EDPSE-02	2. Government Accession No.	3. Recipient's Catalog No.
4. Title and Subtitle **Epoxy Dowel Pile Splice Evaluation**		5. Report Date December 2019- Revised January 2020 6. Performing Organization Code
7. Author(s) Armin Mehrabi https://orcid.org/0000-0003-4736-850X Saman Farhangdoust https://orcid.org/0000-0002-5061-3513		8. Performing Organization Report No.
9. Performing Organization Name and Address Department of Civil and Environmental Engineering Florida International University 10555 West Flagler Street, EC 3680 Miami, FL 33174		10. Work Unit No. (TRAIS) 11. Contract or Grant No. BDV29-977-52
12. Sponsoring Organization Name and Address FDOT Research Center Phone: (850) 414-5260 605 Suwannee Street Tallahassee, Florida 32399-0450 Email: research.center@dot.state.fl.us		13. Type of Report and Period Covered Interim Report- Task 2 Deliverable 14. Sponsoring Agency Code
15. Supplementary Notes		

16. Abstract

The objective of this project is to investigate the behavior and effectiveness of epoxy dowel splice, experimentally and analytically, for prestressed precast concrete piles using corrosion resistant material for dowels (SS, CFRP, and GFRP), and comparing their performance to conventional carbon steel dowel splices. The research project aims to verify the effectiveness of SS and CFRP dowels, and applicability of substitute GFRP dowels as a more economical alternative. It will develop design procedure and details for GFRP epoxy dowel splices, aims at recommending refinements to current designs, and develop design drawings for the recommended details. It will also develop an analytical framework that can be used for design of future variations of pile and splice systems. The primary focus will be on the flexural behavior of the pile splices. This report covers Task 2 of the project which focuses on: Design calculations for the GFRP Epoxy Dowel Pile Splice capacities, and detailed drawings depicting the design for incorporation into the testing phase under Task 3 and 4.

17. Key Words Prestressed Precast Concrete Pile, Pile Splice, Epoxy Dowel Splice, CFRP, HSSS, SS, GFRP,		18. Distribution Statement No Restriction	
19. Security Classification Unclassified	20. Security Classification (of this page) Unclassified	21. No. of Pages 43	22. Price

(this page is intentionally left blank)

Epoxy Dowel Pile Splice Evaluation

Project No. BDV29-977-52

Interim Report – Task 2 Deliverable

December 2019 (Revised January 2020)

Principal Investigator: Armin Mehrabi
Co-PI: David Garber
Co-PI: Seung Jae Lee
Graduate Assistant: Saman Farhangdoust

Department of Civil and Environmental Engineering

Florida International University

Miami, FL

Authors

Saman Farhangdoust
Armin Mehrabi

Sponsored by

Florida Department of Transportation

A report from

FLORIDA INTERNATIONAL UNIVERSITY

Contents

List of Figures

List of Tables

Abstract

The objective of this project is to investigate the behavior and effectiveness of epoxy dowel splice, experimentally and analytically, for prestressed precast concrete piles using corrosion resistant material for dowels (SS, CFRP, and GFRP), and comparing their performance to conventional carbon steel dowel splices. The research project aims to verify the effectiveness of SS and CFRP dowels, and applicability of substitute GFRP dowels as a more economical alternative. It will develop design procedure and details for GFRP epoxy dowel splices, aims at recommending refinements to current designs, and develop design drawings for the recommended details. It will also develop an analytical framework that can be used for design of future variations of pile and splice systems. The primary focus will be on the flexural behavior of the pile splices. This report covers Task 2 of the project which focuses on:

- Design calculations for the GFRP Epoxy Dowel Pile Splice capacities;
- Detailed drawings depicting the design for incorporation into the testing phase under Task 3 and 4.

1 INTRODUCTION

1.1 Problem Statement

Establishing bridge foundations where there is a top layer of weak soils normally requires application of deep foundations such as pile foundation. Driving prestressed-precast concrete piles (PPCP) is one of the options among various types of piles and installation methods. This option provides in many cases an economic and rapid alternative. However, traditional prestressed piles that use carbon steel strands and bars are prone to corrosion, especially when they are in a marine environment. In such environment, alternating water levels and water splash cause deposit and migration of salts into the pile that can accelerate corrosion. Florida Department of Transportation (FDOT) has recently implemented programs to use alternative prestressing strand material that are corrosion resistant. The use of Carbon Fiber Reinforced Polymers (CFRP) and High Strength Stainless Steel (HSSS) for strands and other reinforcement in concrete piles have shown great improvements in the resistance against corrosion.

For various reasons, it often happens that splicing of pile segments has to be performed at the site to achieve longer lengths. The shipping and transportation constraints may limit the length of precast prestressed pile segments that can be delivered to the bridge site. Also, when there is headroom limitation for pile driving, the length of pile segments may be smaller than the length required to establish adequate resistance. In such cases, splicing can be preplanned. Another reason that the pile segments would be less than the length required for resistance is the case of unpredictable soil resistance, which leads to unplanned splicing. Dowel-type splicing using epoxy grout is the focus of this project. In the dowel-type splice, holes are cast or drilled into the top of the lower pile to receive dowel rebars protruding out of the lower end of the upper pile. Dowel rebars can be made of carbon steel as in conventional splicing, or of Stainless Steel (SS), Carbon Fiber Reinforced Polymer (CFRP), or Glass Fiber Reinforced Polymer (GFRP) bars. FDOT has Standard Plans s showing CFRP and SS dowels, but does not cover a GFRP dowel application. Despite occasional use of alternate corrosion resistant dowel splicing, their true behavior is not fully understood yet. Analytical and experimental investigations for structural evaluation of these splices in comparison with splices using conventional bars are scarce.

1.2 Research Objectives

The objective of this project therefore is to investigate the behavior and effectiveness of the epoxy dowel splice for prestressed-precast concrete piles using corrosion resistant material for dowels (SS, CFRP, and GFRP), and comparing their performance to conventional carbon steel dowel splices. The project includes reviewing previous investigations on this subject and design of pile splices according to available codes and analytical models. Pile segments will be fabricated at an approved precast plant, then moved to the FDOT Structures Laboratory, spliced and tested in bending. Using the test results, the project will aim to verify the effectiveness of SS and CFRP dowels, and applicability of GFRP dowels. Design procedure and details will be developed for GFRP epoxy dowel splices, and if applicable, refinements to the current designs for CFRP and SS dowels will be introduced, and design drawings for the recommended details will be developed. It will also develop an analytical framework that can be used in future for systems not covered in this project. The focus of this study will be on the flexural behavior of pile splices.

The objective includes quantifying the effectiveness of the current pile splice details and developing cost-effective versions for corrosion-resistant piles. The research intends to provide a better understanding of the performance and behavior of spliced bearing piles along with a refined design that will be incorporated within the FDOT Standard Plans (Index 455-series).

Task 1 including literature review was completed in July 2019, and the report was submitted to FDOT. This report covers Task 2 of the project which focuses on:

- Design calculations for the GFRP Epoxy Dowel Pile Splice capacities;
- Detailed drawings depicting the design for incorporation into the testing phase under Task 3 and 4.

2 DEVELOPMENT OF EPOXY DOWEL PILE SPLICE DESIGN

In this section, a design for pile splice using GFRP dowels applicable to 18x18-in square piles is proposed. A combination of applicable codes and standards as identified below are used to develop this design. It is realized that GFRP dowels can be used for piles that include corrosion-resistant reinforcement including CFRP and HSSS strands. The focus of this study will be on designing for flexural resistance and checking for other load effects.

Design and construction of the piles will follow the FDOT Structures Manual Volumes 1 (SDG) and 4 (FRPG) [January 2020], FDOT Standard Specification for Road and Bridge Construction [January 2020], and FDOT Standard Plans Index Series 455 [2020]. The FRPG references both the 2018 AASHTO Design Guide Specifications for GFRP-Reinforced Concrete Bridges (AASHTO-GFRP2) and Concrete Bridge Beams Prestressed with CFRP Systems (AASHTO-CFRP1). FDOT Standard Specification for Road and Bridge Construction [January 2020] Section 932 specifies the minimum mechanical properties for both GFRP and CFRP reinforcing, with equivalent limits to ASTM D7957-17 for GFRP reinforcing, but with some enhanced testing criteria for sustained load performance. FDOT Section 933 specifies the minimum mechanical properties for CFRP prestressing strands, while Section 455 requires that pile splices develop the following capacities:

- Axial Compressive Strength = (Pile Cross sectional area) x (28-day concrete strength) = 1944 kips
  Nominal axial strength = 0.85 * 1944 = 1652 kips
- Axial Tensile Strength = (Pile Cross sectional area) x 900 psi = 291.6 kips
- Flexural Strength (Table 1) = 245 (kip-ft)

Table 1: Flexural Capacities Limits *(from FDOT Spec. Section 455.7)*

Pile Size (inches)	Bending Strength (kip-feet)
18	245
24	325
20	600
30	950

2.1 Design of GFRP Dowel

Design and detailing of piles were assumed to follow the FDOT Standard Plans Index No. 455-001 to 018. For the design of pile splice using GFRP Dowels, following assumptions were also made:

- It is assumed that epoxy does not reduce the bond strength of GFRP with concrete. In other words, the bond behavior of GFRP bar with epoxy adhesive is assumed to be the same as GFRP bar embedded directly in concrete,
- A linear relationship for tensile stress-strain for GFRP dowels all the way to rupture,
- The maximum compressive strain in the concrete (strain at crushing) is assumed to be 0.3%
- The most common type of GFRP uses E-glass fiber, but enhanced E-CR (Corrosion Resistant) glass fiber is mandated by FDOT Section 932 and ASTM D7957-17 for internal concrete reinforcing, and assumed for use in splice.
- For the case of pure axial compression, for calculation of the resistance, the gross cross-sectional area of the concrete is conservatively used and contribution of dowel bars are ignored.
- The material and mechanical properties comply with the mechanical properties of FRP reinforcing bars in accordance with Specifications Section 932 for the design of structural concrete [FDOT Standard Specification for Road and Bridge Construction]. Additionally, improved mechanical properties under consideration by ASTM D30 Committee will be evaluated to highlight the potential for improved performance.
- First trial design was adopted based on dowel consisting of GFRP #10 bars. The design is checked for other sizes if applicable. The main goal is to develop a design that is optimized taking account the economy, higher bending strength, and simplicity. The latter would be satisfied especially if a design similar to conventional splices can be used.
- Splice is designed for pure flexure and checked for other combined load effects.

2.1.1 Cross-section physical and mechanical parameters

According to the FDOT Standard Plans Index Series 455-001 and 455-018 [2020], the clear cover for tie is 3-inches (76.2 mm) (Figure 1). Pile cross section including the dowels will be as shown in Figure 2 adopted from FDOT Standard Plans Index Series 455-018 and 455-118 [2020]. Assuming #10 GFRP dowel bars following the pattern in the standard drawings, the clear cover (Eq. 1) and Spacing (Center to center) are 4.865 inch (123.5 mm) and 3.3 inch (83.82 mm), respectively.

Clear cover = FDOT Effective Cover – 1/2* bar diameter #10 = 5.5 - (1.27/2) = 4.865” (1)

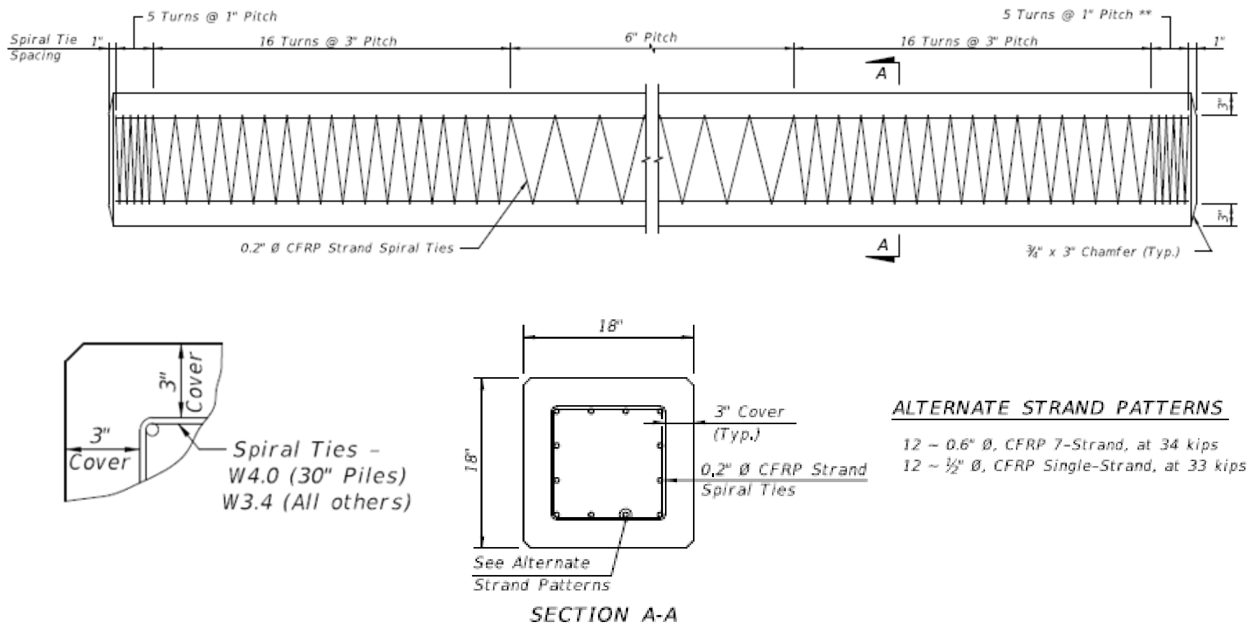

Figure 1: The typical cover of FDOT pre-design pile [FDOT Standard Plans Index Series 455-100]

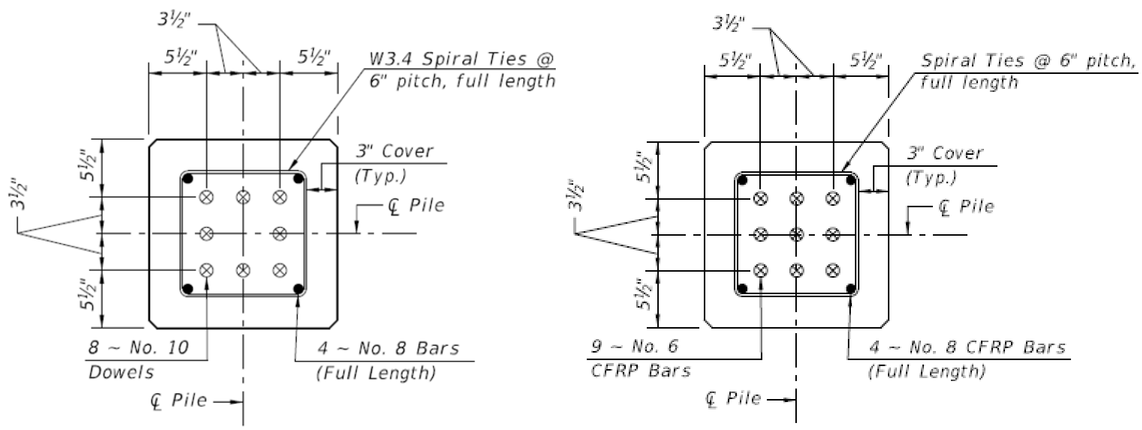

Figure 2: The typical pile cross section for steel bars (left) and CFRP bars (right)

According to the FDOT Standard Specifications for Road and Bridge Construction (January 2020), section properties of FRP reinforcing bars shall meet the requirements in Table 2. Improved minimum mechanical properties are currently being considered by an ASTM D30 Committee working group for 20%-30% improved Modulus of Elasticity and Guaranteed Tensile Strength (GTS). For this report, a higher modulus (E_f = 8,500 ksi) and GTS of 83 kips, 102.5 kips, 123 kips for #8, #9, and #10 bars, respectively, are also used reflecting the proposed (2021) improved properties.

Table 2: Sizes and tensile loads of FRP bars

Bar Size Designation	Nominal Bar Diameter (in)	Nominal Cross Sectional Area (in^2)	Measured Cross-Sectional Area (in^2)		Minimum Guaranteed Tensile Load (kips)	
			Minimum	Maximum	GFRP Bars	CFRP Bars
2	0.250	0.049	0.046	0.085	6.1	10.3
3	0.375	0.11	0.104	0.161	13.2	20.9
4	0.500	0.20	0.185	0.263	21.6	33.3
5	0.625	0.31	0.288	0.388	29.1	49.1
6	0.750	0.44	0.415	0.539	40.9	70.7
7	0.875	0.60	0.565	0.713	54.1	-
8	1.000	0.79	0.738	0.913	66.8	-
9	1.128	1.00	0.934	1.137	82.0	-
10	1.270	1.27	1.154	1.385	98.2	-

As per FDOT Standard Plans Index 455-001, the type of concrete for pile should be Class V (Special). According to the concrete classes and strength included in the FDOT Structures Manual Volume 1 [January 2020], the minimum 28-day compressive strength (f'_c) is considered 6 (ksi) for concrete Class V (Special) (Table 3). The yield strength of steel (f_y), minimum ultimate tensile strength of strands, and other properties for section analysis are adopted from FDOT Standard Plans Index 455-000 series.

Table 3: FDOT concrete classes and strengths

Class II	3.4
Class II (Bridge Deck)	4.5
Class III	5.0
Class III (Seal)	3.0
Class IV	5.5
Class IV (Drilled Shaft)	4.0
Class V (Special)	6.0
Class V	6.5
Class VI	8.5

GFRP bars are manufactured from two main parts of fibers and matrix resin. The former part provides strength and stiffness, and the matrix of FRP protects and transfers stresses between fibers. Many researchers have analyzed the mechanical and material properties of GFRP rebars in the past years. Different types of GFRP bars have been summarized by Fu et al. [2019] (Figure 3).

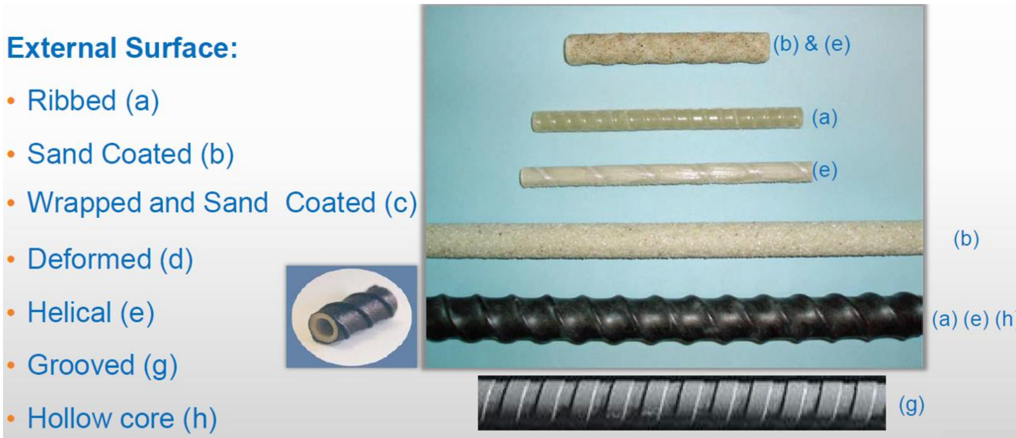

Figure 3: Different types of FRP [Fu et al. 2019]

E-glass fiber is considered the most common type used in GFRP for composite reinforcement having favorable electrical insulating properties, low susceptibility to moisture, and at the same time, high mechanical properties [ACI 440.R-07]. Recently, the durability benefits of E-CR (Corrosion Resistant) glass fibers has been recognized and mandated for internal concrete reinforcing bars under ASTM D7957-17. S-glass fibers provide for higher strength but are associated with higher costs. Figure 4 shows the stress-strain difference between FRPs and steel.

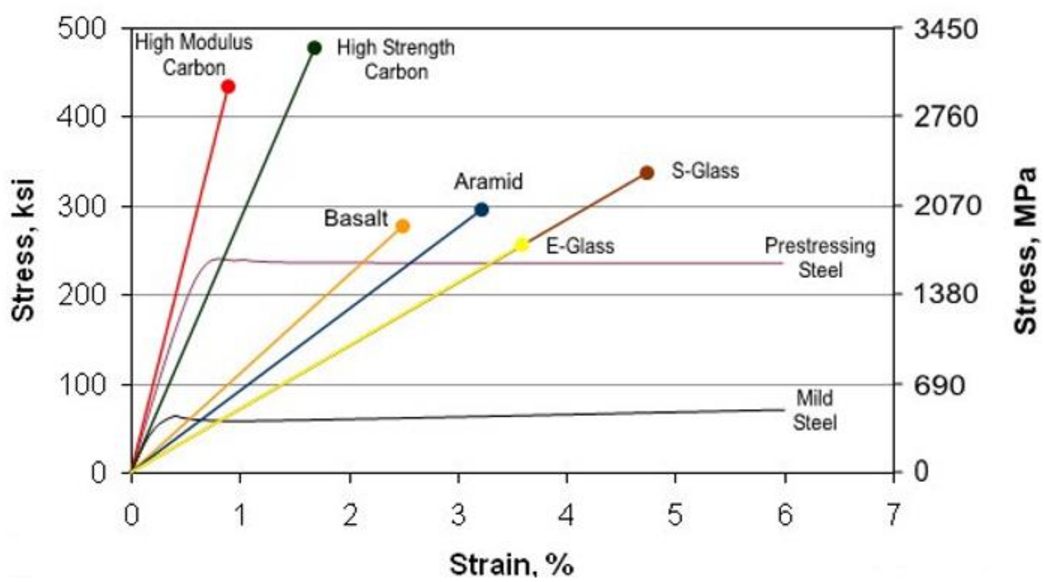

Figure 4: The stress–strain curves of FRPs and steel [Prince Engineering]

As it is shown in this figure, FRP material shows a linear elastic behavior all the way to rupture. Moreover, the GFRP has a lower strain and higher ultimate strength compared to steel.

In the following sections, the resistance of the pile splice with GFRP dowels will be first calculated using the current (2020) GFRP properties for different arrangement of bars and sizes. Then, for each case, the pure flexural resistance that is the basis for the design of splice in this report will also be calculated using the proposed (2021) GFRP properties.

2.1.2 Pile Splice using 8-GFRP Bars # 10 as Dowels

As it was mentioned earlier, as first trial (consistent with steel dowel design), 8-GFRP bar #10 is considered as dowels in the pile splice section. The cross-sectional area and minimum guaranteed (nominal) tensile load are selected from Table 2 per FDOT requirement to be 1.27 sq.in. and 98.2 kips. The guaranteed tensile strength, f_{fu}^{*} , therefore is calculated to be 77.56 ksi. Design tensile strength of FRP, defined as the guaranteed tensile strength multiplied by the environmental reduction factor, $f_{fu} = C_E f_{fu}^{*}$. C_E is the environmental reduction factor selected here to be 0.7 because pile structure is exposed to earth [ACI 440.1R-15]. Therefore, $f_{fu} = 54.29\ ksi$. The Modulus of Elasticity, E_f , is adopted from ACI 440.1R.15 (Table 7.2.1) to be 6,500 ksi. Accordingly, the design rupture strain (ε_{fu}) is calculated to be 0.0083. A section analysis by hand calculation was carried out to check the flexural resistance (Table 1) in accordance with ACI 440.1R-15. The analysis was performed to obtain:

A. Axial compression strength,
B. Axial tension strength,
C. Balanced failure point,
D. Pure flexural moment strength.

2.1.2.1 Balanced Failure

At the balanced failure point, concrete crushing and FRP rupture are assumed to occur simultaneously (Figure 5). At the balanced failure mode, the concrete reaches its ultimate in compression and the FRP bars in the farthest layer reaches the design rupture strain at the same time. The distance of the center of each of the three dowel layers to the upper edge of the section is calculated as:

$$d_1 = 5.5 \text{ in } (139.7 \text{ mm}) \tag{2}$$

$$d_2 = 9 \text{ in } (228.6 \text{ mm}) \tag{3}$$

$$d_3 = 12.5 \text{ in } (317.5 \text{ mm}) \tag{4}$$

The position of the neutral axis C is calculated using the equation below 3.3 (84 mm).

$$\frac{0.003}{C} = \frac{0.0083}{d_3 - C} \tag{5}$$

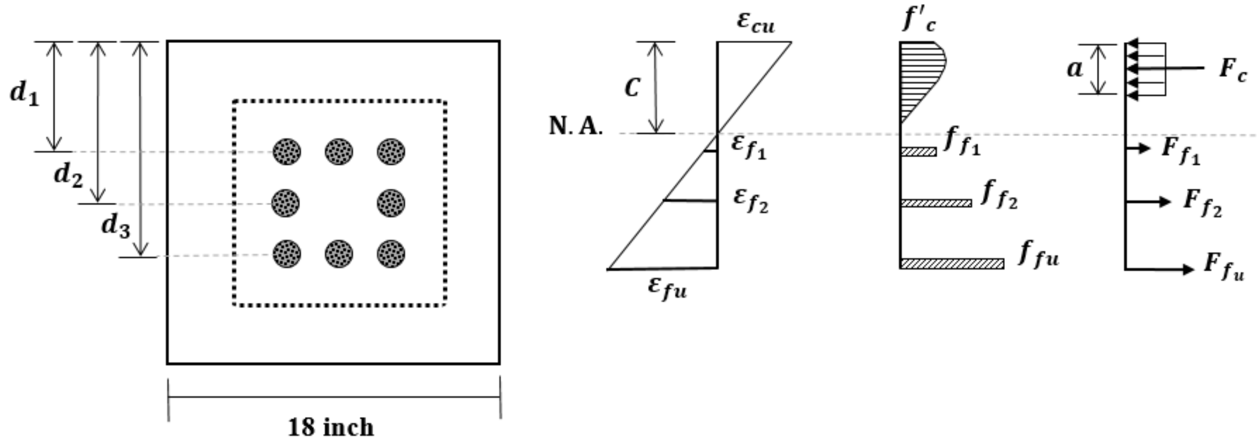

Figure 5: Strain and stress distribution at the balanced failure mode

Accordingly, based on the strain and stress conditions for balanced failure mode displayed in Figure 5, the compressive force of concrete and tension force of GRFP dowels were calculated by:

$$F_c = \alpha * f'_c * \beta * C * b = 0.85 * 6 * 0.75 * 3.3 * 18 = 227.42 \text{ kips} \tag{6}$$

$$f_{f_1} = [\varepsilon_{f_1}] * E_f = \left[\left(\frac{5.5-3.3}{3.3}\right) * 0.003\right] * 6500 = 12.96 \text{ ksi} < f_{fu} \tag{7}$$

$$F_{f_1} = f_{f_1} * A_{G1} = 12.96 * 3.81 = 49.25 \text{ kips} \quad \text{Tension} \tag{8}$$

$$f_{f_2} = [\varepsilon_{f_2}] * E_f = \left[\left(\frac{9-3.3}{3.3}\right) * 0.003\right] * 6500 = 33.62 \text{ ksi} < f_{fu} \tag{9}$$

$$F_{f_2} = f_{f_2} * A_{G2} = 33.62 * 2.54 = 85.16 \text{ kips} \quad \text{Tension} \tag{10}$$

$$F_{f_3} = F_{f_u} = f_{fu} * A_{G1} = 54.11 * 3.81 = 206.22 \text{ kips} \quad \text{Tension} \tag{11}$$

As a result, the force and moment of the balanced point due to the strain compatibility and force equilibrium are calculated as follows:

$$\begin{cases} P_n = 227.42 - (206.22 + 85.16 + 49.25) = -113.21 \text{ kips} \\ M_n = -172.405 + 1765.13 + 721.77 = 2314.49 \text{ k.in} = 192.874 \text{ k.ft} \end{cases} \quad (12)$$

2.1.2.2 Axial Compression Strength

The pure compression point is the second design parameter that needs to be calculated for analyzing the M-N interaction of FRP- based pile splice. According to the Figure 6, the strain of GFRP dowels ε_f cannot exceed the maximum compressive strain in the concrete (0.003). Therefore, the total compression force will be: $F_{Totol} = (N * \varepsilon_f * E_{fc} * A_G) + (\alpha * f'_c * [(a * b) - N * A_G])$, but is conservatively taken as the resistance of the gross section of concrete area: $\alpha * f'_c * a * b = 1652.4$ kips.

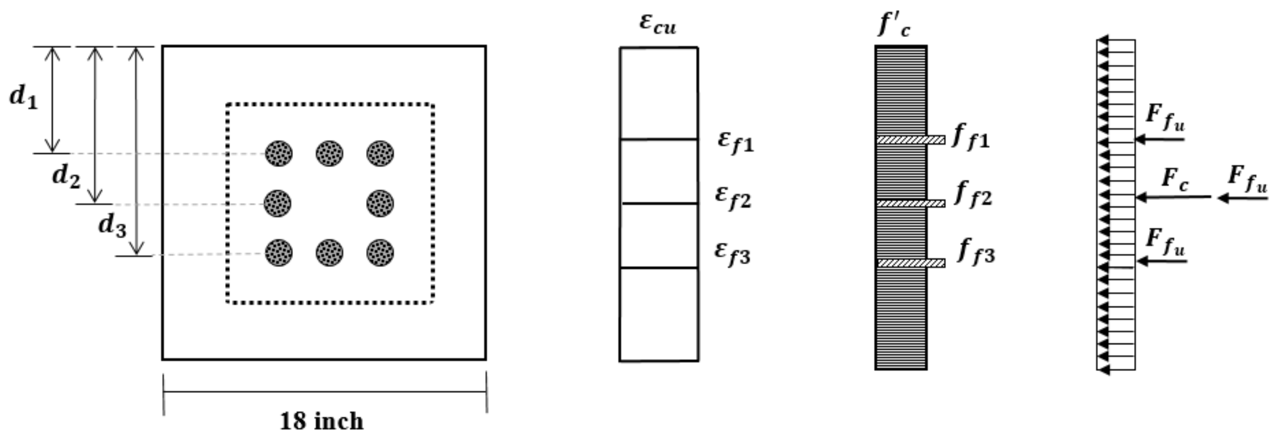

Figure 6: Strain and stress distribution at the pure compression mode (theoretical)

2.1.2.3 Axial Tensile Strength

According to Figure 7, concrete does not contribute to tensile strength, therefore, axial tensile strength will include the tensile strength of all eight dowels at design tensile strength, f_{fu}. Therefore, the total compression force will be:

$$F_{Totol} = (N * f_{fu} * A_G) = (8 * 54.29 * 1.27) = -549.92 \text{ kips} \quad (13)$$

Axial tensile strength is greater than required nominal strength of 291 kips.

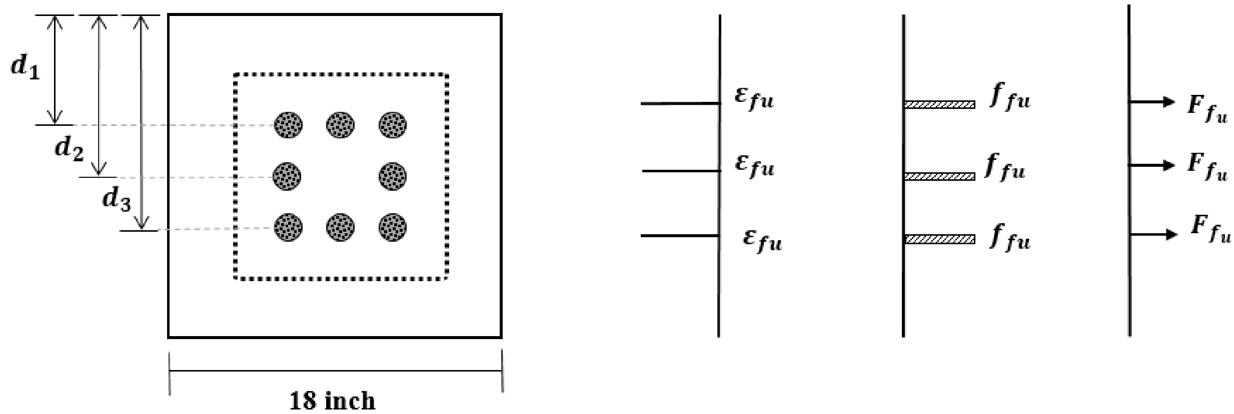

Figure 7: Strain and stress distribution at the pure tension mode

2.1.2.4 Pure Flexural Moment Strength

The pure flexural moment strength (no axial force) is governed by concrete crushing. At this mode of failure, the strain compatibility and force equilibrium is assumed for the pile splice section shown in Figure 8.

$$F_c = \alpha * f'_c * \beta * b * C = 0.85 * 6 * 0.75 * 18 * C \quad (14a)$$

$$F_{f_1} = [\varepsilon_{f_1}] * E_f * A_{G1} = \left[\left(\frac{5.5-C}{C}\right) * 0.003\right] * 6500 * 3.8 \quad (15a)$$

$$F_{f_2} = [\varepsilon_{f_2}] * E_f * A_{G2} = \left[\left(\frac{9-C}{C}\right) * 0.003\right] * 6500 * 2.53 \quad (16a)$$

$$F_{f_3} = [\varepsilon_{f_3}] * E_f * A_{G3} = \left[\left(\frac{12.5-C}{C}\right) * 0.003\right] * 6500 * 3.8 \quad (17a)$$

As it was discussed earlier, the pure flexural moment strength is also calculated for the proposed (2021) improved GFRP rebar properties:

$$F_c = \alpha * f'_c * \beta * b * C = 0.85 * 6 * 0.75 * 18 * C \quad (14b)$$

$$F_{f_1} = [\varepsilon_{f_1}] * E_f * A_{G1} = \left[\left(\frac{5.5-C}{C}\right) * 0.003\right] * 8500 * 3.8 \quad (15b)$$

$$F_{f_2} = [\varepsilon_{f_2}] * E_f * A_{G2} = \left[\left(\frac{9-C}{C}\right) * 0.003\right] * 8500 * 2.53 \quad (16b)$$

$$F_{f_3} = [\varepsilon_{f_3}] * E_f * A_{G3} = \left[\left(\frac{12.5-C}{C}\right) * 0.003\right] * 8500 * 3.8 \quad (17b)$$

After simplification, the following set of equations for forces in concrete and dowel layers are calculated based on the depth to the neutral axis C:

Current (2020) GFRP properties

$$\begin{cases} F_c = 68.85 * C \\ F_{f_1} = 74.1\left(\frac{5.5-C}{C}\right) \\ F_{f_2} = 49.4\left(\frac{9-C}{C}\right) \\ F_{f_3} = 74.1\left(\frac{12.5-C}{C}\right) \end{cases} \tag{18a}$$

Proposed (2021) GFRP properties

$$\begin{cases} F_c = 68.85 * C \\ F_{f_1} = 96.85\left(\frac{5.5-C}{C}\right) \\ F_{f_2} = 64.57\left(\frac{9-C}{C}\right) \\ F_{f_3} = 96.85\left(\frac{12.5-C}{C}\right) \end{cases} \tag{18b}$$

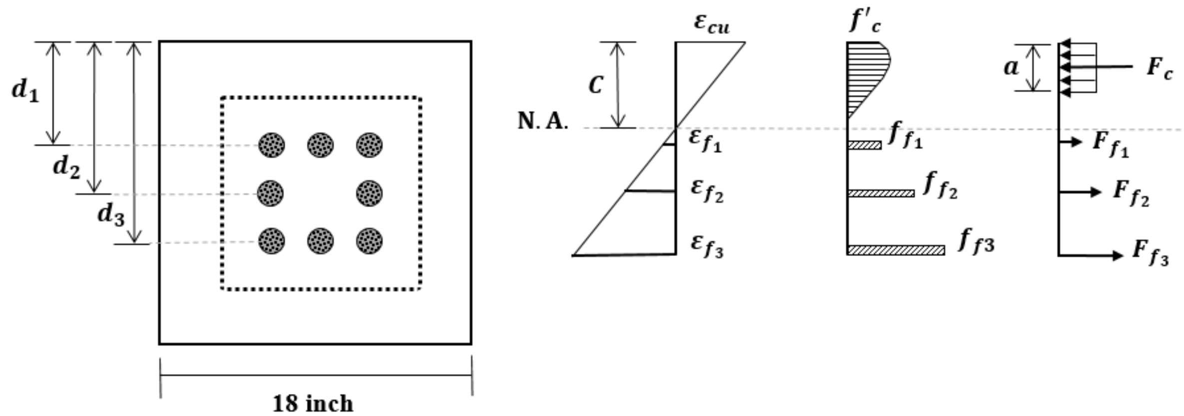

Figure 8: Strain and stress distribution at the concrete crushing failure mode

At the pure flexure point, $F_c = \sum F_{fi}$. As a result, the value of C for current and proposed ones, respectively, were found 3.84 in (97.5 mm) and 4.23 in (107.4 mm) as the depth to the neutral axis. Because the neutral axis is above all the FRP bars, all the dowel levels are in tension. Accordingly, the moment resistance of pile splice section and stress of three level GFRP dowels will be as by calculation 19a.

For the proposed improved GFRP rebar properties, the moment resistance is also shown in calculation 19b:

Current (2020) GFRP properties

$$\begin{cases} f_{f_1} = -8.4 \text{ ksi} \\ f_{f_2} = -26.1 \text{ ksi} \\ f_{f_3} = -43.9 \text{ ksi} \\ M_{n\#10} = \sum F_i * Y_i = 2472.9 \text{ k}-\text{in} = 206.1 \text{ k}-\text{ft} \end{cases} \tag{19a}$$

Proposed (2021) GFRP properties

$$\begin{cases} f_{f_1} = -7.6 \text{ksi} \\ f_{f_2} = -28.7 \text{ ksi} \\ f_{f_3} = -49.8 \text{ ksi} \\ M_{n\#10} = \sum F_i * Y_i = 2720.2 \text{ k}-\text{in} = 226.7 \text{ k}-\text{ft} \end{cases} \tag{19b}$$

According to the above, the nominal moment resistance, M_n , was calculated to be 206.1 k-ft and 226.7 k-ft for 8-GFRP #10 dowels based on the current and proposed GFRP properties, respectively. This result shows this pile splice with 8-GFRP #10 dowels is able to develop 84% and 92 % required moment resistance (Table 1), respectively, based on the current and proposed GFRP properties. The stress in the farthest bars is less than the design strength of the GFRP, therefore, the section fails with concrete crushing that is a desirable mode. Comparison using the design moment resistance will be carried out later in this report.

2.1.3 Pile Splice Using 8-GFRP Bars #8 as Dowel

Because the maximum stress in the GFRP dowel bar is less than the maximum strength specified for GFRP, it is only prudent to try a smaller size of GFRP bar. Therefore, a set of 8-GFRP #8 bars in three layers, with the same arrangement as the #10s was also examined for the pile splice. For the selected product, the cross-sectional area and minimum guaranteed (nominal) tensile load are selected from Table 2 per FDOT requirement to be 0.785 in^2 and 66.8 kips. For the GFRP dowels based on the current (2020) properties, the guaranteed tensile strength, f_{fu}^* , therefore is calculated to be 85.09 ksi. Design tensile strength of FRP, defined as the guaranteed tensile strength multiplied by the environmental reduction factor, $f_{fu} = C_E f_{fu}^*$. C_E is the environmental reduction factor selected here to be 0.7 because pile structure is exposed to earth [AASHTO-GFRP2/ACI 440.1R-15]. Therefore, $f_{fu} = 59.56\ ksi$. The Modulus of Elasticity, E_f , is adopted from FDOT Spec 932-/ASTM D7957-17 to be 6500 ksi. A section analysis for the pure flexural bending strength was carried out in accordance with AASHTO-GFRP2 to check the moment resistance of pile splice using #8 GFRP bars. The failure is assumed to occur with crushing of concrete. The strain compatibility for the pile splice section is as shown in Figure 8.

$$F_c = \alpha * f'_c * \beta * b * C = 0.85 * 6 * 0.75 * 18 * C \tag{20a}$$

$$F_{f_1} = [\varepsilon_{f_1}] * E_f * A_{G1} = \left[\left(\frac{5.5-C}{C}\right) * 0.003\right] * 6500 * 2.35 \tag{21a}$$

$$F_{f_2} = [\varepsilon_{f_2}] * E_f * A_{G2} = \left[\left(\frac{9-C}{C}\right) * 0.003\right] * 6500 * 1.57 \tag{22a}$$

$$F_{f_3} = [\varepsilon_{f_3}] * E_f * A_{G3} = \left[\left(\frac{12.5-C}{C}\right) * 0.003\right] * 6500 * 2.35 \tag{23a}$$

Similar calculations for the proposed (2021) improved GFRP rebar properties show:

$$F_c = \alpha * f'_c * \beta * b * C = 0.85 * 6 * 0.75 * 18 * C \tag{20b}$$

$$F_{f_1} = [\varepsilon_{f_1}] * E_f * A_{G1} = \left[\left(\frac{5.5-C}{C}\right) * 0.003\right] * 8500 * 2.35 \tag{21b}$$

$$F_{f_2} = [\varepsilon_{f_2}] * E_f * A_{G2} = \left[\left(\frac{9-C}{C}\right) * 0.003\right] * 8500 * 1.57 \tag{22b}$$

$$F_{f_3} = [\varepsilon_{f_3}] * E_f * A_{G3} = \left[\left(\frac{12.5-C}{C}\right) * 0.003\right] * 8500 * 2.35 \tag{23b}$$

After simplification, section forces of the pile splice is calculated based on the depth to the neutral axis C:

Current (2020) GFRP properties

$$\begin{cases} F_c = 68.85 * C \\ F_{f_1} = 45.92\left(\frac{5.5-C}{C}\right) \\ F_{f_2} = 30.61\left(\frac{9-C}{C}\right) \\ F_{f_3} = 45.92\left(\frac{12.5-C}{C}\right) \end{cases}$$

(24a)

Proposed (2021) GFRP properties

$$\begin{cases} F_c = 68.85 * C \\ F_{f_1} = 60.05\left(\frac{5.5-C}{C}\right) \\ F_{f_2} = 40.03\left(\frac{9-C}{C}\right) \\ F_{f_3} = 60.05\left(\frac{12.5-C}{C}\right) \end{cases}$$

(24b)

To investigate the pure flexural point, $F_c = \sum F_{fi}$ should be considered as the force equilibrium equition. As a result, the depth to the neutral axis C for current and proposed properties, respectively, were found to be 3.20 in (81.3 mm) and 3.55 in (90.2 mm). Accordingly, the moment of pile splice section and stress of three level GFRP dowels will be:

Current (2020) GFRP properties

$$\begin{cases} f_{f_1} = -13.92 \text{ ksi} \\ f_{f_2} = -35.18 \text{ ksi} \\ f_{f_3} = -56.45 \text{ ksi} \\ M_{n\#8} = \sum F_i * Y_i = 2073.3 \text{ k}-\text{in} = 172.7 \text{ k}-\text{ft} \end{cases}$$

(25a)

Proposed (2021) GFRP properties

$$\begin{cases} f_{f_1} = -13.92 \text{ ksi} \\ f_{f_2} = -39 \text{ ksi} \\ f_{f_3} = -64.09 \text{ ksi} \\ M_{n\#8} = \sum F_i * Y_i = 2291.3 \text{ k}-\text{in} = 190.9 \text{ k}-\text{ft} \end{cases}$$

(25b)

The nominal moment resistance for the pile section using 8-GFRP #8 bars in three layers, M_n, was calculated to be 172.7 k-ft and 190.9 k-ft based on the current and proposed GFRP properties, respectively. This result shows the pile splice with 8-GFRP #8 dowels is able to develop 70% and 78% of the required moment resistance (Table 1), respectively, based on the current and proposed GFRP properties.

The stress in the farthest bars is less than the design strength of the GFRP (but closer than that of 8-#10 bars), therefore, the section fails with concrete crushing. Comparison using the design moment resistance will be carried out later in this report.

2.1.4 Pile Splice using 9-GFRP Bars #10 as Dowels

As the next trial, 9-GFRP bars #10 is selected as a replacement for CFRP dowels in FDOT Standard Plans Index Series 455-118 [2020]. For the GFRP bars, the cross-sectional area and minimum guaranteed (nominal) tensile load are selected from Table 2 per FDOT requirement to be 1.27 in2 and 98.2 kips. The design tensile strength of FRP, f_{fu} is 54.29 ksi. The Modulus of Elasticity, E_f , is also adopted from FDOT Spec 932-3/ASTM D7957-17 to be 6500 ksi. As the pure flexural moment resistance (no axial force) is governed by concrete crushing, the failure is assumed to occur with crushing of concrete. At this mode of failure, the strain compatibility and force equilibrium is assumed for the pile splice section shown in Figure 9.

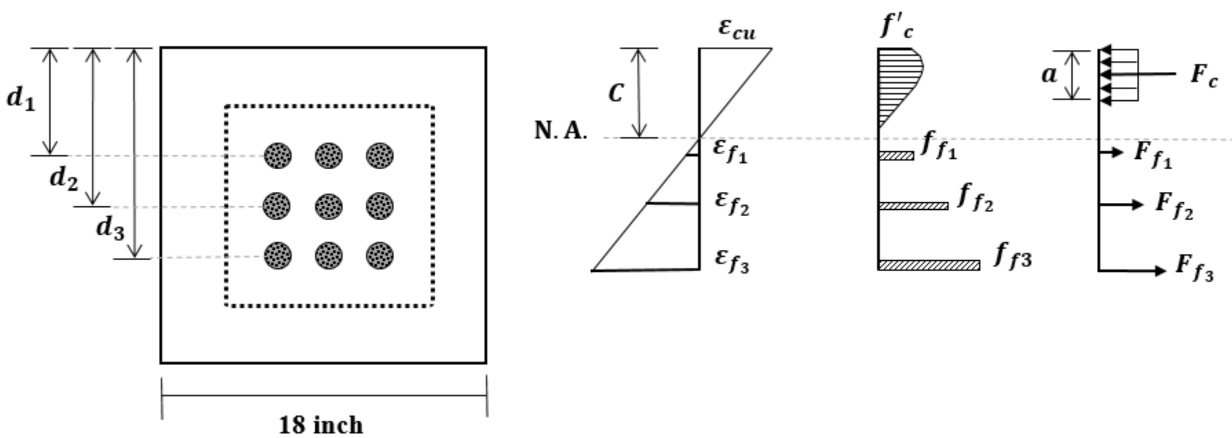

Figure 9: Strain and stress distribution at the concrete crushing failure mode

A section analysis for the pure flexural bending strength was carried out in accordance with AASHTO-GFRP2 to check the moment strength resistance of pile splice using 9-GFRP dowels #10:

$$F_c = \alpha * f'_c * \beta * b * C = 0.85 * 6 * 0.75 * 18 * C \quad (26a)$$

$$F_{f_1} = [\varepsilon_{f_1}] * E_f * A_{G1} = \left[\left(\frac{5.5-C}{C}\right) * 0.003\right] * 6500 * 3.8 \quad (27a)$$

$$F_{f_2} = [\varepsilon_{f_2}] * E_f * A_{G2} = \left[\left(\frac{9-C}{C}\right) * 0.003\right] * 6500 * 3.8 \quad (28a)$$

$$F_{f_3} = [\varepsilon_{f_3}] * E_f * A_{G3} = \left[\left(\frac{12.5-C}{C}\right) * 0.003\right] * 6500 * 3.8 \quad (29a)$$

Similar calculations for the proposed improved GFRP rebar properties show:

$$F_c = \alpha * f'_c * \beta * b * C = 0.85 * 6 * 0.75 * 18 * C \tag{26b}$$

$$F_{f_1} = \left[\varepsilon_{f_1}\right] * E_f * A_{G1} = \left[\left(\frac{5.5-C}{C}\right) * 0.003\right] * 8500 * 3.8 \tag{27b}$$

$$F_{f_2} = \left[\varepsilon_{f_2}\right] * E_f * A_{G2} = \left[\left(\frac{9-C}{C}\right) * 0.003\right] * 8500 * 3.8 \tag{28b}$$

$$F_{f_3} = \left[\varepsilon_{f_3}\right] * E_f * A_{G3} = \left[\left(\frac{12.5-C}{C}\right) * 0.003\right] * 8500 * 3.8 \tag{29b}$$

After simplification, the following set of equations for forces in concrete and dowel layers are calculated based on the depth to the neutral axis C, for both material options:

Current (2020) GFRP properties

$$\begin{cases} F_c = 68.85 * C \\ F_{f_1} = 74.1\left(\frac{5.5-C}{C}\right) \\ F_{f_2} = 74.1\left(\frac{9-C}{C}\right) \\ F_{f_3} = 74.1\left(\frac{12.5-C}{C}\right) \end{cases}$$

(30a)

Proposed (2021) GFRP properties

$$\begin{cases} F_c = 68.85 * C \\ F_{f_1} = 96.86\left(\frac{5.5-C}{C}\right) \\ F_{f_2} = 96.86\left(\frac{9-C}{C}\right) \\ F_{f_3} = 96.85\left(\frac{12.5-C}{C}\right) \end{cases}$$

(30b)

At the pure flexure point, $F_c = \sum F_{fi}$. As a result, the value of C for the current and proposed ones, respectively, were calculated to be 4.01 in (101.8 mm) and 4.40 in (111.76 mm) as the depth to the neutral axis. Because the neutral axis is above all the FRP bars, all the dowel levels are in tension. Accordingly, the moment of pile splice section and stress of three level GFRP dowels will be:

Current (2020) GFRP properties

$$\begin{cases} f_{f_1} = -7.23 \text{ ksi} \\ f_{f_2} = -24.24 \text{ ksi} \\ f_{f_3} = -41.25 \text{ ksi} \\ M_{n\#10} = \sum F_i * Y_i = 2522.8 \text{ k.in} = 210.2 \text{ k.ft} \end{cases} \tag{31a}$$

Proposed (2021) GFRP properties

$$\begin{cases} f_{f_1} = -6.34 \text{ ksi} \\ f_{f_2} = -26.61 \text{ ksi} \\ f_{f_3} = -46.87 \text{ ksi} \\ M_{n\#10} = \sum F_i * Y_i = 2767 \text{ k.in} = 230.6 \text{ k.ft} \end{cases} \tag{31b}$$

According to the above, the nominal moment resistance, M_n, for the pile section using 9-GFRP #10 bars in three layers was calculated to be 210.2 k-ft and 230.6 k-ft based on the current and proposed GFRP properties, respectively. This result shows the pile splice with 9-GFRP #10 dowels is able to develop 86% and 94% of the required moment resistance (Table 1), respectively, based on the current and proposed

GFRP properties. A comparison between splice with 8 #10 and 9 #10 bars indicates that addition of one bar increases the nominal flexural resistance only by 2 percent. Comparison using the design moment resistance will be carried out later in this report.

2.1.5 Pile Splice Using 9-GFRP Bars #8 as Dowel

Because the maximum stress in the GFRP dowel bar is less than the maximum strength specified for GFRP, it is only prudent to try a smaller size of GFRP bar. Therefore, a set of 9-GFRP #8 bars in three layers was also examined for the pile splice. For this case study, the cross-sectional area and minimum guaranteed (nominal) tensile load are selected from Table 2 per FDOT requirement to be 0.785 in^2 and 66.8 kips. The design tensile strength of FRP, f_{fu} is 59.56 ksi. The Modulus of Elasticity, E_f , is also adopted from AASHTO-GFRP2/ASTM D7957-17 to be 6500 ksi. A section analysis for the pure flexural bending strength was carried out in accordance with AASHTO-GFRP2to check the moment strength resistance of pile splice using 9-GFRP dowels of #8. The failure is assumed to occur with crushing of concrete. The strain compatibility for the pile splice section is as shown in Figure 9.

$$F_c = \alpha * f'_c * \beta * b * C = 0.85 * 6 * 0.75 * 18 * C \quad (32a)$$

$$F_{f_1} = [\varepsilon_{f_1}] * E_f * A_{G1} = \left[\left(\frac{5.5-C}{C}\right) * 0.003\right] * 6500 * 2.35 \quad (33a)$$

$$F_{f_2} = [\varepsilon_{f_2}] * E_f * A_{G2} = \left[\left(\frac{9-C}{C}\right) * 0.003\right] * 6500 * 2.35 \quad (34a)$$

$$F_{f_3} = [\varepsilon_{f_3}] * E_f * A_{G3} = \left[\left(\frac{12.5-C}{C}\right) * 0.003\right] * 6500 * 2.35 \quad (35a)$$

Similar calculations for the proposed improved GFRP rebar properties show:

$$F_c = \alpha * f'_c * \beta * b * C = 0.85 * 6 * 0.75 * 18 * C \quad (32b)$$

$$F_{f_1} = [\varepsilon_{f_1}] * E_f * A_{G1} = \left[\left(\frac{5.5-C}{C}\right) * 0.003\right] * 8500 * 2.35 \quad (33b)$$

$$F_{f_2} = [\varepsilon_{f_2}] * E_f * A_{G2} = \left[\left(\frac{9-C}{C}\right) * 0.003\right] * 8500 * 2.35 \quad (34b)$$

$$F_{f_3} = [\varepsilon_{f_3}] * E_f * A_{G3} = \left[\left(\frac{12.5-C}{C}\right) * 0.003\right] * 8500 * 2.35 \quad (35b)$$

After simplification, section forces of the pile splice is calculated based on the depth to the neutral axis C:

Current (2020) GFRP properties

$$\begin{cases} F_c = 68.85 * C \\ F_{f_1} = 45.92\left(\frac{5.5-C}{C}\right) \\ F_{f_2} = 45.92\left(\frac{9-C}{C}\right) \\ F_{f_3} = 45.92\left(\frac{12.5-C}{C}\right) \end{cases}$$

(36a)

Proposed (2021) GFRP properties

$$\begin{cases} F_c = 68.85 * C \\ F_{f_1} = 60.05\left(\frac{5.5-C}{C}\right) \\ F_{f_2} = 60.05\left(\frac{9-C}{C}\right) \\ F_{f_3} = 60.05\left(\frac{12.5-C}{C}\right) \end{cases}$$

(36b)

To investigate the pure flexural point, $F_c = \sum F_{fi}$ should be considered as the force equilibrium equation. As a result, the depth to the neutral axis C for the current and proposed ones, respectively, were calculated to be 3.36 in (85.34 mm) and 3.71 in (94.23 mm) which shows all the dowel levels are in tension mode as we expected. Accordingly, the moment of pile splice section and stress of three level GFRP dowels will be:

Current (2020) GFRP properties

$$\begin{cases} f_{f_1} = -\,12.42\ \mathrm{ksi} \\ f_{f_2} = -\,32.74\ \mathrm{ksi} \\ f_{f_3} = -53.05\ \mathrm{ksi} \\ M_{n\#8} = \sum F_i * Y_i = 2125.23\ \mathrm{k.in} = 177.1\ \mathrm{k.ft} \end{cases} \quad (37a)$$

Proposed (2021) GFRP properties

$$\begin{cases} f_{f_1} = -12.22\ \mathrm{ksi} \\ f_{f_2} = -36.23\ \mathrm{ksi} \\ f_{f_3} = -60.24\ \mathrm{ksi} \\ M_{n\#8} = \sum F_i * Y_i = 2342.6\ \mathrm{k.in} = 195.2\ \mathrm{k.ft} \end{cases} \quad (37b)$$

The nominal moment resistance, M_n, for the pile section using 9-GFRP #8 bars in three layerswas calculated to be 177.1 k-ft and 195.2 k-ft based on the current and proposed GFRP properties, respectively. This result shows the pile splice with 9-GFRP #8 dowels is able to develop 72% and 80% of the required moment resistance (Table 1), respectively, based on the current and proposed GFRP properties. A comparison between splice with 8-#8 and 9-#8 bars indicates that addition of one bar increases the nominal flexural resistance only by 2 percent. Comparison using the design moment resistance will be carried out later in this report.

2.1.6 Design Moment Strength

According to ACI 440.1R-15 [2015] and AASHO-GFRP2 [2018], the design flexural strength of an FRP-reinforced section dependents on whether it is controlled by concrete crushing or FRP rupture. This can be determined by comparing the FRP reinforcement ratio, ρ_f, to the balanced reinforcement ratio ρ_{fb}. Accordingly, there are three possible failures for pile splice:

- Balanced failure condition (concrete crushing and FRP rupture occurs at the same time)
- Failure governed by concrete crushing (concrete crushing occurs before FRP rupture)
- Failure governed by FRP rupture (FRP rupture occurs before concrete crushing)

According to ACI 440.1R-15, for a single-layer GFRP tension reinforcement, balanced reinforcement ratio can be calculated using the equations below:

$$\rho_{fb} = \left(\alpha_1 \beta_1 \frac{f'_c}{f_{fu}}\right)\left(\frac{E_f \varepsilon_{cu}}{E_f \varepsilon_{cu} + f_{fu}}\right) \tag{38}$$

$$\rho_f = \frac{A_f}{bd} \tag{39}$$

Where A_f refers to the area of three bars in the single layer reinforcement farthest from compression zone. It is structurally advantageous for a concrete section reinforced with FRP that concrete crushes first, i.e., FRP reinforcement ratios is larger than the balanced ratio. In AASHTO-GFRP2, the balanced reinforcement is expressed in terms of strain and defined as Compression-Controlled or Tensioned-Controlled with a Transition zone due expected variations in material properties. If the reinforcement ratios are equal to balanced reinforcement ratio, the failure is balanced. If $\rho_f \geq \rho_{fb}$, then the failure will be initiated by crushing of concrete, and the nominal moment strength will be calculated for the case of single-layer tension reinforcement by:

$$M_n = A_f f_f \left(1 - 0.59 \frac{\rho_f f_f}{f'_c}\right) d^2 \tag{40}$$

However, if $\rho_f < \rho_{fb}$, then the flexural failure will be governed by rupture of FRP bar, and the nominal moment strength for the case of single-layer reinforcement will be calculated by:

$$M_n = A_f f_{fu} \left(d - \frac{\beta_1 C_b}{2}\right) \tag{41}$$

As it is shown in Figure 10, according to the Sec. 2.5.5.2 of the AASHTO-GFRP2, for the case of single-layer GFRP tension reinforcement, the resistance factor can be calculated by (42). The tensioned-controlled resistance factor is slightly less conservative than the ACI 440.1R-15 strength reduction factor, based on more recent comparative reliability analysis:

$$\phi = \text{Resistance Factor (for strength)} = \begin{cases} 0.55 & \text{for } \varepsilon_{ft} = \varepsilon_{fd} \; (Tension - Controlled) \\ 0.75 & \text{for } \varepsilon_{ft} \le 0.80\varepsilon_{fd} \; (Compression - Controlled) \\ 1.55 - \frac{\varepsilon_{ft}}{\varepsilon_{fd}} & \text{For } \; 0.80\varepsilon_{fd} < \varepsilon_{ft} < \varepsilon_{fd} \; (Transition) \end{cases} \quad (42)$$

Where the $\varepsilon_{fd} = C_E\varepsilon_{fu}$ is design rupture strain and ε_{fu} is guaranteed rupture strain from AASHTO. It should be noted that different terminology has been used by ACI 440.1R-15 and AASHTO-GFRP2 to describe the design rupture strain and guaranteed rupture strain. To clarify, the ε_{fd} and ε_{fu} used by AASHTO correspond to ε_{fu} and ε_{fu}^{*} used by ACI 440.1R-15, respectively.

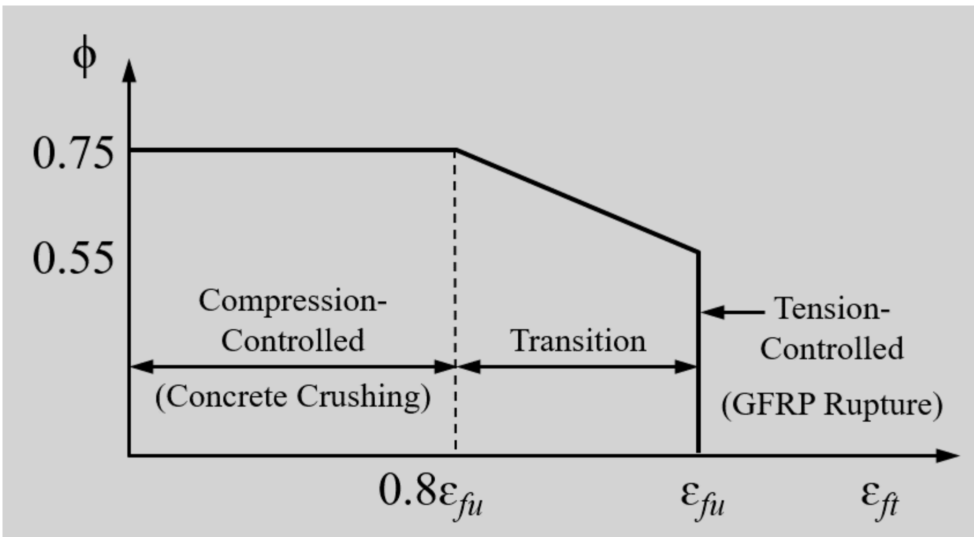

Figure 10: Strength Limit State resistance factor [AASHTO-GFRP2]

Table 4 shows the strength resistance factor, ϕ, corresponding to #8 and #10 bars for two different number of bars at pure flexural moment based on conditions set by Eq. 42 (AASHTO).

When using the current (2020) GFRP properties, the ratio of $^{\varepsilon_t}/_{\varepsilon_{fd}}$, for #10 bars is 0.80 for 8 number of bars and 0.76 for 9 number of bars. Therefore, for both cases, the strength resistance factor, ϕ , for pure bending of a pile splice for Sections using #10 bars can be taken as 0.75. Similarly, for #8 bars, the ratio of $^{\varepsilon_t}/_{\varepsilon_{fd}}$ for 8 and 9 number of bars, respectively, are 0.95 and 0.89. Therefore, the strength resistance factor, ϕ , for pure bending for a pile splice using #8 bars is calculated as 0.60 and 0.66, respectively for 8 and 9 number of bars..

Table 4: The resistance factor for current (2020) GFRP properties

Design	Number of Bars	ε_t	ε_{fd}	$\varepsilon_t/\varepsilon_{fd}$	ϕ
With GFRP Dowel #10	**8**	**0.00675**	**0.00835**	**0.80**	**0.75**
	9	**0.00635**	**0.00835**	**0.76**	**0.75**
With GFRP Dowel #8	**8**	**0.00868**	**0.00916**	**0.95**	**0.60**
	9	**0.00816**	**0.00916**	**0.89**	**0.66**

For the proposed (2021) GFRP properties, the strength resistance factor, ϕ, corresponding to #8 and #10 bars for 8 and 9 number of bars at pure flexural moment is calculated and shown in Table 5.

Table 5: The resistance factor for proposed (2021) GFRP properties

Design	Number of Bars	ε_t	ε_{fd}	$\varepsilon_t/\varepsilon_{fd}$	ϕ
With GFRP Dowel #10	**8**	**0.00586**	**0.008**	**0.73**	**0.75**
	9	**0.00551**	**0.008**	**0.69**	**0.75**
With GFRP Dowel #8	**8**	**0.00754**	**0.00871**	**0.86**	**0.68**
	9	**0.00709**	**0.00871**	**0.81**	**0.74**

2.1.6.1 Design Moment Strength for the Case of 8-GFRP Dowels

For a pile splice using three layers of 8-GFRP bars # 10, based on the calculated resistance factor, the failure will be governed by concrete crushing, and the resistance factor ϕ will be 0.75. Hence, the factored flexural moment will be:

$$\mathrm{M_{u\#10}} = \phi \mathrm{M_{n\#10}} = \begin{cases} \mathit{Current}\ (2020): 0.75 * 206.1\ = 154.57\ \mathrm{K-ft} \\ \mathit{Proposed}\ (2021): 0.75 * 226.7\ = 170.02\ \mathrm{K-ft} \end{cases} \tag{43}$$

In the same manner, for a pile splice using three layers of 8-GFRP # 8 bars, the design flexural moment will be:

$$\mathrm{M_{u\#8}} = \phi \mathrm{M_{n\#8}} = \begin{cases} \mathit{Current}\ (2020): 0.60 * 172.7\ = 103.62\ \mathrm{K-ft} \\ \mathit{Proposed}\ (2021): 0.68 * 190.9\ = 129.81\ \mathrm{K-ft} \end{cases} \tag{44}$$

2.1.6.2 The Case of 9-GFRP Dowels

For a pile splice using three layers of GFRP # 10 bars, based on the modified resistance factor, the failure will be governed by concrete crushing, and the resistance factor ϕ will be 0.75. Therefore, the factored flexural resistance will be:

$$\mathrm{M}_{\mathrm{u\#10}} = \phi\mathrm{M}_{\mathrm{n\#10}} = \begin{cases} \mathit{Current}\ (2020): 0.75 * 210.2\ = 157.65\ \mathrm{K-ft} \\ \mathit{Proposed}\ (2021): 0.75 * 230.6\ = 172.95\ \mathrm{K-ft} \end{cases} \tag{45}$$

In the same manner, for a pile splice using three layers of GFRP # 8 bars, the design flexural moment will be:

$$\mathrm{M}_{\mathrm{u\#8}} = \phi\mathrm{M}_{\mathrm{n\#8}} = \begin{cases} \mathit{Current}\ (2020): 0.66 * 177.1\ = 116.89\ \mathrm{K-ft} \\ \mathit{Proposed}\ (2021): 0.74 * 195.2\ = 144.45\ \mathrm{K-ft} \end{cases} \tag{46}$$

As it shown in Tables 6 and 7, comparing two cases of #8 and #10 bars, the use of both 8 and 9-GFRP #10 bars can provide a better design for pile splice because it provides for significantly higher resistance and more importantly, the design with #10 bars are more consistent with conventional design used by FDOT (Figure 2). It is realized that the splice design moment strength provided by GFRP #10 bars is lower than that required by Standard Specification for Road and Bridge Construction [January 2020], however, it is believed that the use of larger diameter bars as well as the use of larger number of dowels on each side of the section are not practical and will create spacing and installation issues.

Table 6: Comparison between bending moment strength and required moment strength for GFRP dowels of different sizes (current 2020 specifications)

Design	Nominal Moment Strength (k-ft)	Design Moment Strength (k-ft)	FDOT Required Moment Resistance (k-ft)	Ratio of Nominal Moment Strength to Required (Nominal)	Ratio of Design Moment Strength to Required (Design)
With 8-GFRP Dowel #10	206.1	154.57	**245**	**84%**	**63%**
With 8-GFRP Dowel #8	172.7	103.62	**245**	**70%**	**42%**
With 9-GFRP Dowel #10	210.2	157.65	**245**	**86%**	**64%**
With 9-GFRP Dowel #8	177.1	116.89	**245**	**72%**	**48%**

Table 7: Comparison between bending moment strength and required moment strength for GFRP dowels of different sizes (proposed 2021 specifications)

Design	Nominal Moment Strength (k-ft)	Design Moment Strength (k-ft)	FDOT Required Moment Resistance (k-ft)	Ratio of Nominal Moment Strength to Required (Nominal)	Ratio of Design Moment Strength to Required (Design)
With 8-GFRP Dowel #10	226.7	170.02	**245**	**92%**	**69%**
With 8-GFRP Dowel #8	190.9	129.81	**245**	**78%**	**53%**
With 9-GFRP Dowel #10	230.6	172.95	**245**	**94%**	**71%**
With 9-GFRP Dowel #8	195.2	144.45	**245**	**80%**	**59%**

For the current (2020) GFRP properties- The results show that 8-GFRP #10 bars in three layers can develop 84% and 63% of the required moment resistance (Table 1) when using the nominal moment resistance and design moment resistance, respectively. Moreover, these results show a pile splice with 9-GFRP #10 bars in three layers can develop 86% and 64% of the required moment resistance (Table 1) when using the nominal moment resistance and design moment resistance, respectively.

For the proposed (2021) GFRP properties- The results show that 8-GFRP #10 bars in three layers can develop 92% and 69% of the required moment resistance (Table 1) when using the nominal moment resistance and design moment resistance, respectively. Moreover, these results show a pile splice with 9-GFRP #10 bars in three layers can develop 94% and 71% of the required moment resistance (Table 1) when using the nominal moment resistance and design moment resistance, respectively.

It should also be noted that the capacities calculated using the available design codes have proven to result in extremely conservative estimation. This can be verified later in this report with the section analysis using Response 2000, as well as with the experimental evaluations planned for this project. <u>From this point on, the splice design configuration using 8-#10 bars will be used for detailing and other considerations.</u> This configuration provides the consistency of design with steel counterpart as well as near maximum strength (only up to 2 percent lower than 9-#10).

2.2 GFRP Dowel Detailing for Preplanned Pile Splice

Similar to the design of existing pile splice details reflected in the FDOT Standard Plan Index 455-102, the detailing of the pile splice using GFRP dowel bars will require calculation of two lengths; one is the development length of strand used inside the pile segments, and the other is lap splice length for GFRP bar dowel. The strand development length needs to be defined since for developing the full resistance of the pile beyond the splice section in the upper segment, the GRFP dowel will need to extend and overlap along that length with the strand. The lap splice length for dowel needs to be determined since for the splice to develop its full resistance, the dowel shall be inserted in the lower pile segment with that length to splice with the auxiliary bar already embedded in the lower pile segment. Lap splice length in turn is calculated based on the development length of GFRP bar in concrete. Development length in general depends on confinement, bar surface roughness and shape, embedment length, type of concrete, concrete compressive strength. Development length for strand and lap splice length for GFRP bar is calculated in the following sections.

2.2.1 Strand – Development Length

2.2.1.1 Steel Strand

Although GFRP dowels are not intended to be used with conventional steel reinforced piles, for completeness as well as to use for Stainless-Steel reinforcing case, development and lap splice lengths are calculated for conventional steel. ACI 318R-14 and AASHTO LRFD Bridge Design-8th Edition were used to calculate the development length and lap splice of steel strands in pile. The specified jacking force in FDOT Standard Plans for steel strand of 0.6-inch diameter is 35 kips, which gives an initial stress in the strand of 161.3 ksi (35 kips / 0.217 in^2). Fifteen (15) percent loss is assumed to determine the effective stress in the prestressing strands (based on Young and Ge, 2018).

2.2.1.1.1 ACI 318R-14

Based on section of 25.4.8.1 of the ACI 318R-14, the development for pretensioned seven wire strands of pile in tension was calculated by:

$$l_d = \left(\frac{f_{se}}{3}\right) d_b + \left(\frac{f_{ps} - f_{se}}{1}\right) d_b \tag{47}$$

Where

- f_{se} (the effective stress in prestressing reinforcement) = 85% f_{pi} = 137.1 ksi (assuming 15% loss) [Young and Ge 2018]
- f_{pi} (jacking stress or initial stress) = 161.3 ksi
- f_{pu} (Minimum guaranteed ultimate strength) = 270 ksi [Young and Ge 2018]
- f_{ps} (stress in strand at flexural failure of beam)= $f_{pu}\left(1-\frac{\gamma_p \rho_p f_{pu}}{\beta_1 f_c'}\right) = 270\left(1-\frac{0.28*0.0032*270}{0.75*6}\right)$ =255.4 ksi

In which,

$\rho_p = \frac{A_{\rho s}}{bd_p} = \frac{0.86}{18*(14.5)}$=0.0032

$d_p = 18 - 0.3\ (\text{half of strand diam.}) - 0.2(\text{wire spiral diam.}) - 3(\text{clear cover}) = 14.5$

$A_{\rho s} = 4 * 0.217\ (\text{strand area}) = 0.86$

$\gamma_p = 0.28$ (typical low relaxation strand)

$\beta_1 = 0.85 - \left(0.05 * (f_c' - 4)\right) = 0.75$

Accordingly, development length is calculated to be 98.4 in. For 0.5 in.-diameter strands used in 18x18 in. piles for 16-0.5-in strand configuration, this development length is calculated to be 80.25 in. Normally, the larger of these two development lengths is used in the design. However, since GFRP dowels will be used only with 16-0.5-in. HSSS strand configuration in the pile (FDOT Standard Plans Index 455-118), the 80.25 in. (6' 9") development length will be used for GFRP splice design in HSSS pile option.

2.2.1.1.2 AASHTO

Based on section 5.9.4.3.2 of AASHTO LRFD Bridge Design-8th Edition, the development length of pretensioning strand is calculated by:

$$l_d \geq k\left(f_{ps} - \frac{2}{3} f_{pe}\right) d_b \tag{48}$$

Where

- k is1 for piling with a depth smaller than 24 is (in old version of AASHTO this factor was 1.6),
- f_{ps} (stress in strand at flexural failure of beam)
- f_{pe} (the effective stress in prestressing reinforcement) = f_{se} above

$$l_d \geq 1\left(255.4 - \frac{2}{3}137.1\right)0.6 = 98.4\ \text{in.} \tag{49}$$

Development length for steel strand from both ACI and AASHTO Specification are identical.

2.2.1.2 HSSS Strand

Paul et al. (2015) demonstrated through testing that transfer and development length for HSSS-2205 prestressing strands are considerably smaller than that predicted by AASHTO LRFD, the flexural and shear strengths of piles using SS were greater than predicted by both ACI-318 and AASHTO LRFD, and the stress loss was smaller than that predicted by AASHTO LRFD refined method. These properties were not affected after installation and extraction. Also, Mullins et al. (2014) demonstrated that transfer and development lengths of HSSS strands are not longer than comparable conventional carbon steel strands. Accordingly, the development length of HSSS strand will be considered to be the same as the conventional steel strand.

2.2.1.3 CFRP Strand

The AASHTO-CFRP1 was used to calculate the development length and lap splice for CFRP strands in tension. The equation used is based on Section 6-2 of the ACI 440.4R-04 with unit conversion coefficients, the recommended equation for development length can be calculated using Eq. (50);

$$L_d = L_t + L_{fb} \tag{50}$$

Where L_t and L'_t , respectively, were calculated by:

$$L_t = \frac{(f_{pe})d_b}{\alpha_t(f'_c)^{0.67}} \tag{51}$$

$$L_{fb} = \frac{(f_{\rho u} - f_{pe})d_b}{\alpha_{fb}(f'_c)^{0.67}} \tag{52}$$

Where:

f'_c= Concrete strength at time of loading

$f_{\rho u}$= Ultimate tensile strength of the CFCC

f_{pe}= Effective prestressing stress

α_{fb}= Factor for the flexural bond length of FRP tendon

α_t= Factor for the transfer length of FRP tendon

As a result, the development length of prestressing strand of pile in tension will be calculated by:

$$L_d = \frac{(f_{pe})d_b}{\alpha_t\left(f_c'\right)^{0.67}} + \frac{(f_{\rho u} - f_{pe})d_b}{\alpha_{fb}\left(f_c'\right)^{0.67}} \quad (53)$$

It has been observed that there are some idiosyncrasies with these development length equations when the strand is not pretensioned to near the maximum permitted transfer limits, which is sometime the case for FDOT square piles where 1000 psi residual compression is the controlling design condition.

Figure 11 shows the available Commercial CFRP prestressing tendons under the brand names of Carbon Fiber Composite Cable (CFCC) by Tokyo Rope (Japan) [Roddenberry et al. 2014]. Figure 12 shows recently published updates to the CFCC minimum specifications.

Designation (Configuration diameter) 呼称		Diameter 直径 (mm)	Effective cross sectional area 有効断面積 (mm²)	Guaranteed capacity 保証破断荷重 (kN)	Nominal mass density* 単位長さ質量 (g/m)	Tensile elastic modulus* 弾性係数 (kN/mm²)
	U 5.0φ	5.0	15.2	38	30	167
	1×7 7.5φ	7.5	31.1	76	60	155
	1×7 10.5φ	10.5	57.8	141	111	155
	1×7 12.5φ	12.5	76.0	184	145	155
	1×7 15.2φ	15.2	115.6	270	221	155
	1×7 17.2φ	17.2	151.1	350	289	155
	1×19 20.5φ	20.5	206.2	316	410	137
	1×19 25.5φ	25.5	304.7	467	606	137
	1×19 28.5φ	28.5	401.0	594	777	137
	1×37 35.5φ	35.5	591.2	841	1,185	127
	1×37 40.0φ	40.0	798.7	1,200	1,529	145

Figure 11: CFCC standard specification [Roddenberry et al. 2014]

Shape of cross section	Standard specification of CFCC									
	Designation	Diameter	Effective cross sectional area		Guaranteed capacity		Nominal mass density		Tensile elastic modulus	
		inch	mm²	in²	kN	kip	g/m	lb/ft	kN/mm²	ksi
○	CFCC U 5.0 φ	0.20	15.9	0.025	40.4	9.1	30	0.020	167	24,221
	CFCC 1×7 7.9 φ	0.31	31.1	0.048	79.3	17.8	60	0.040	155	22,481
	CFCC 1×7 10.8 φ	0.43	57.8	0.090	147.2	33.1	112	0.075	155	22,481
	CFCC 1×7 12.5 φ	0.49	75.6	0.117	192.5	43.3	146	0.098	155	22,481
	CFCC 1×7 15.2 φ	0.60	115.6	0.179	294.4	66.2	223	0.150	155	22,481
	CFCC 1×7 17.2 φ	0.68	151.1	0.234	385.0	86.6	292	0.196	155	22,481

Figure 12: CFCC standard specification [Yamamoto, 2019]

The development length analysis was carried out for CFRP strand pattern shown in FDOT Standard Plans 2020 (455-118) for 0.6-inch diameter strand. As it is shown in Figure 1, the pile uses 12-0.6-inch diameter CFRP strands. According to Section 933 of the FDOT Standard Specification for Road and Bridge Construction [January 2020], the nominal cross sectional area of the CFRP 0.6-inch diameter strand is considered to be 0.179 inches (Table 8).

Table 8: Different sizes and loads of current CFRP prestressing strands and bars

Type	Nominal Diameter (in)	Nominal Cross Sectional Area (in^2)	Nominal Ultimate Load (P_u) (kips)	Nominal Ultimate Tensile Stress (ksi)
Single Strand - 5.0mm Ø	0.20	0.030	9	300
7-strand - 7.5mm Ø	0.30	0.050	17	340
7-strand - 10.5mm Ø	0.41	0.090	32	356
Single Strand - 9.5mm Ø	0.38	0.110	35	318
7-strand - 12.5mm Ø	0.49	0.118	41	347
Single Strand - 12.7mm Ø	0.50	0.196	59	301
7-strand - 15.2mm Ø	0.60	0.179	61	341
19-strand - 20.5mm Ø	0.81	0.320	71	222
7-strand - 17.2mm Ø	0.68	0.234	79	338
19-strand - 25.5mm Ø	1.00	0.472	105	222
19-strand - 28.5mm Ø	1.12	0.621	134	216
37-strand - 35.5mm Ø	1.40	0.916	189	206
37-strand - 40.0mm Ø	1.57	1.240	270	218

The specified jacking force in FDOT Standard Plans for CFCC strand of 0.6-inch diameter is 34 kips, which gives an initial stress in the strand of 189.9 ksi (34 k/0.179 in^2). Fifteen (15) percent loss is assumed to determine the effective stress in the prestressing strands (Young and Ge, 2018). All required information for development length calculations are:

- f_c'= 6 ksi,
- $f_{\rho u}$= 341 ksi [Young and Ge 2018],
- f_{pi}=189.9 ksi
- f_{pe}= 161.5 ksi (assuming loss of 15%) [Young and Ge 2018],
- α_{fb}= 14.8 (inch-pound units) for CFCC [ACI 440.4R-04],
- α_t= 25.3 (inch-pound units) for CFCC [ACI 440.4R-04].

As a result, the development length of the CFRP strand will be:

$$L_d = \frac{161500 * 0.6}{25.3 * (6000)^{0.67}} + \frac{(341000 - 161500) * 0.6}{14.8 * (6000)^{0.67}} = 11.6 + 22.0 = 33.6'' \quad (54)$$

There have been several investigations on determining the development length for CFCC strands. Table 9 summarizes the results of some of these investigations (Roddenberry et al. 2014).

According to these results, the development length of CFCC can be as low as 33.6 in. and as high as 49 in. A consistent value for development length of CFCC cannot be established from the available literature, and experimental evaluation is needed to derive such. For the time being, for a preplanned splice using CFCC strand and GFRP dowel, the dowel length inside the lower pile segment will be taken consistent with the current design of FDOT (Index 455-102) that is 54 in. without the use of auxiliary bars in the lower segment.

Table 9: Development length predictions

Reference	Predicted Length (in.)
Roddenberry et al. (2014)	< 72
Mahmoud and Rizkalla (1996)	29
Mahmoud and Rizkalla (1996) with Grace (2000) α_t	49
Calculated in this report using ACI 440.4R-04	33.6

Furthermore, Table 10 shows recently proposed specification revisions to FDOT Section 933 incorporating the improved CFCC properties for July 2020.

Table 10: CFRP proposed revisions for FDOT Spec 932 standard specification [Knight, 2019]

Typical Sizes and Loads of CFRP Prestressing Strands and Bars				
Type	Nominal Diameter (in)	Nominal Cross Sectional Area (in^2)	Nominal Ultimate Load (P_u) (kips)	Nominal Ultimate Tensile Stress (ksi)
Single Strand-5.0mm Ø	0.20	0.025	9.1	364
7-Strand-7.9mm Ø	0.31	0.048	17.8	370
7-Strand-10.8mm Ø	0.43	0.090	33.1	367
Single Strand-9.5mm Ø	0.38	0.110	35.0	318
7-Strand-12.5mm Ø	0.49	0.117	43.3	370
Single Strand-12.7 mm Ø	0.50	0.196	59.0	301
7-Strand-15.2mm Ø	0.60	0.179	66.2	369
7-Strand-17.2mm Ø	0.68	0.234	86.6	338

If these changes apply, the development length for CFRP strand calculated by Eq. 54 will change to 36.3 in.

2.2.2 Development and Lap Splice Lengths for 8-GFRP #10 Bars

2.2.2.1 Calculation Assuming a Single layer of GFRP Dowel

The standard specification of AASHTO LRFD Bridge Design Guide Specifications for GFRP-Reinforced Concrete – 2nd Edition was used to calculate the development length and lap splice of and GFRP Dowel in pile splice. This calculation is performed for GFRP with both current and proposed/improved properties. Based on Section 2.9.7.4.1-1 of the AASHTO, for deformed FRP bars, the development length in tension can be calculated using Eq. 55.

$$l_d \geq \max\left\{\frac{31.6\alpha\frac{f_{fr}}{\sqrt{f'_c}}-340}{13.6+\frac{C}{d_b}}d,\ 20*d\right\} \qquad (55)$$

Where

f_{fr} = Minimum { f_f and f_{fd} } (56)

The GFRP stress at the time of concrete crushing (bending failure), f_f, is calculated by Eq. (57) assuming a single-layer reinforcement in tension.

$$f_f = \sqrt{\frac{(E_f \varepsilon_{cu})^2}{4} + \frac{0.85\beta_1 f'_c E_f \varepsilon_{cu}}{\rho_f}} - 0.5E_f\varepsilon_{cu} \quad (57)$$

$$= \begin{cases} \textit{Current}\ (2020)\ \textit{GFRP properties}: \sqrt{\frac{(6500*0.003)^2}{4} + \frac{0.85*0.75*6*6500*0.003}{0.0169}} - 0.5*6500*0.003 = 57.40\ \text{ksi} \\ \textit{Proposed}\ (2021)\ \textit{GFRP properties}: \sqrt{\frac{(8500*0.003)^2}{4} + \frac{0.85*0.75*6*8500*0.003}{0.0169}} - 0.5*8500*0.003 = 64.28\ \text{ksi} \end{cases}$$

Where:

$$E_f = \begin{cases} 6500\ ksi\ \ for\ current\ properties\ \ (FDOT\ Section\ 932-3\ /ASTM\ D7957-17) \\ 8500\ ksi\ \ for\ proposed-improved\ properties \end{cases}$$

$\rho_f = \frac{A_f}{bd} = 0.0169$ (GFRP reinforcement ratio assuming single layer with 3 bars)

$A_f = 3.81 in^2$ (Assuming the area of 3 GFRP reinforcement)

$\beta_1 = \max\left\{0.65; 0.85 - 0.05\left(\frac{f'_c}{1000} - 4\right)\right\} = 0.75$

$\alpha = 1$ (Bar location modification factor)

C = 1.75 (Half of the center-to-center spacing of the bars being developed)

In addition, the maximum strength of GFRP bar, f_{fd} , is calculated by:

<u>Current (2020) GFRP properties</u>

$f_{fd} = C_E * f^*_{fu}$ = 0.7 * 77.56 = 54.29 (ksi)

(58-a)

<u>Proposed (2021) GFRP properties</u>

$f_{fd} = C_E * f^*_{fu}$ = 0.7 * (123 / 1.27) = 67.79 (ksi)

(58-b)

In which, f_{fu} depends on the size and the type of GFRP bar (E-CR glass of #10 was picked for our calculations). C_E is the environmental reduction factor selected here to be 0.7 because pile structure is exposed to earth.

Therefore, according to Eq. 59 below, f_{fr} will be 54.29 ksi and 64.28 ksi for the current and the proposed GFRP properties, respectively.

Current (2020) GFRP properties

$$f_{fr} = \min\begin{cases} f_f = 54.40 \text{ ksi} \\ f_{fd} = 54.29 \text{ ksi} \end{cases} \tag{59-a}$$

Proposed (2021) GFRP properties

$$f_{fr} = \min\begin{cases} f_f = 64.28 \text{ ksi} \\ f_{fd} = 67.79 \text{ ksi} \end{cases} \tag{59-b}$$

As a result, the development length for GFRP bar at pile splice in tension, l_d, for the current and proposed GFRP properties will be, respectively, 30.55 in (0.77 m) and 41.48 in (1.05m) by:

$$\begin{cases} \mathit{Current}\ (2020)\ \mathit{GFRP}: l_d \geq \max\left\{\dfrac{31.6 * 1 * \dfrac{54.29}{\sqrt{6}} - 340}{13.6 + \dfrac{1.75}{1.27}} * 1.27, \quad 20 * 1.27\right\} = \max\{30.55'', 25.4''\} = 30.55'' \\ \mathit{Proposed}\ (2021)\ \mathit{GFRP}: l_d \geq \max\left\{\dfrac{31.6 * 1 * \dfrac{64.28}{\sqrt{6}} - 340}{13.6 + \dfrac{1.75}{1.27}} * 1.27, \quad 20 * 1.27\right\} = \max\{41.48'', 25.4''\} = 41.48'' \end{cases}$$

Accordingly, based on the Section 2.9.7.6 of the AASHTO-GFRP2, the lap splice of GFRP deformed bar in tension is calculated to be 40 in (1.00 m) and 54 in (1.4 m), respectively, for the current and proposed GFRP properties using Eq. 60.

Current (2020) GFRP properties

$$\text{lap splice length} = 1.3 * l_d = 39.71'' \cong 40 \text{ in} \tag{60-a}$$

Proposed (2021) GFRP properties

$$\text{lap splice length} = 1.3 * l_d = 53.93'' \cong 54 \text{ in} \tag{60-b}$$

Consider: Given that the adhesive dowels are not touching the strands (non-contact splice), and the surrounding concrete is not interrupted, the use of a 1.3 factor may not be necessary and only the additional offset length (approximately 2-inches) need be added to the basic development length. Additionally, the high degree of confinement offered by the spiral reinforcing at 1-in. and 3-in. spacing near the head and tip of the pile provide enhanced bond development.

2.2.2.2 Calculation for Three layers of GFRP Dowel

The development length calculated in the previous section assumed one layer of reinforcement for calculating the stress level at bars. Since the splice is actually designed using three layers of GFRP dowels (Figure 2), and as such, the actual configuration needs to be considered in calculating the development length and lap splice for GFRP bars. To calculate the development length of GFRP bars, it is necessary to calculate the stress in GFRP at the point of bending failure of pile splice governed by concrete crushing. According to earlier calculation, the actual stress in GFRP and maximum moment strength at crushing of concrete are:

Current (2020) GFRP properties

$$\begin{cases} f_{f_1} = -8.4 \text{ ksi} \\ f_{f_2} = -26.1 \text{ ksi} \\ f_{f_3} = -43.9 \text{ ksi} \\ M_{n\#10} = \sum F_i * Y_i = 2472.9 \text{ k} - \text{in} = 206.1 \text{ k} - \text{ft} \end{cases}$$

Proposed (2021) GFRP properties

$$\begin{cases} f_{f_1} = -7.6 \text{ ksi} \\ f_{f_2} = -28.7 \text{ ksi} \\ f_{f_3} = -49.8 \text{ ksi} \\ M_{n\#10} = \sum F_i * Y_i = 2720.2 \text{ k} - \text{in} = 226.7\text{k} - \text{ft} \end{cases}$$

Similar to the development length calculation for one-layer reinforcement in AASHTO, development length for the case of three layers of reinforcement is calculated by considering $f_f = f_{f3}$ (Eq. 61).

Accordingly, f_{fr} is calculated to be 43.9 ksi and 49.8 ksi, respectively, for the current and proposed GFRP properties using Eq. 59.

Current (2020) GFRP properties

$$f_{fr} = \min \begin{cases} f_f = f_{f3} = 43.9 \text{ ksi} \\ f_{fd} = 54.29 \text{ ksi} \end{cases}$$

(61-a)

Proposed (2021) GFRP properties

$$f_{fr} = \min \begin{cases} f_f = f_{f3} = 49.8 \text{ ksi} \\ f_{fd} = 67.79 \text{ ksi} \end{cases}$$

(61-a)

Therefore, the development length for GFRP bars in tension, l_d, can be calculated to be $\text{Max}\{19.19", 25.4"\} = 25.4$ in (0.64 m) and $\text{Max}\{20.19", 25.4"\} = 25.4$ in (0.64 m) for the current and proposed GFRP properties, respectively.

Accordingly, the lap splice of the deformed bar in tension for both current and proposed GFRP properties will be calculated to be 33.02 in. (0.84 m).

Nevertheless, to be conservative and to allow the GFRP bars to develop their maximum strength, the lap splice length calculated based on developing full strength, i.e., 40-inches for current and 54-inches for proposed properties, is recommended for the design of pile splice using GFRP dowels.

It should also be noted that often, it is expected that the concrete will develop strengths considerably higher than specified, therefore, allowing GFRP dowels to develop stresses larger than that calculated for pure bending assuming the nominal concrete strength.

2.2.3 Ultimate Bond Stress for 8-GFRP Dowel #10

The bond stress, τ, of the GFRP dowels (Figure 13) can be calculated according to Section 10.1 of the ACI 440.1R.15, by :

$$l_e \pi \mathrm{d}_b \tau = A_{f,bar} f_{fu} \quad (62)$$

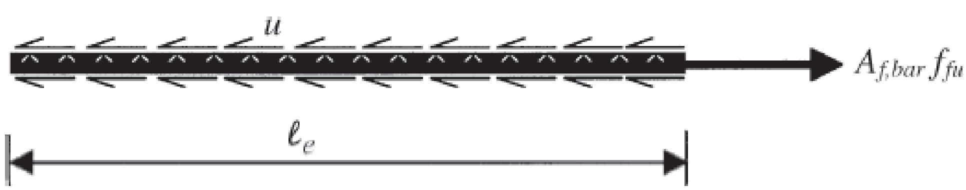

Figure 13: Transfer of force through bond of the concrete and The GFRP dowels

The embedded length of the GFRP bar, l_e, is equal to the proposed development length for GFRP dowel in previous section. Embedded length and other properties were selected for GFRP bar #10.

As a result, the bond stress is:

$$\tau = \frac{A_{f,bar} f_{fu}}{l_d \pi \mathrm{d}_b} = \frac{1.27 * 54.11}{40 * 3.14 * 1.27} = \frac{53.8}{131.6} = 430.8 \text{ psi} \quad (63)$$

The ultimate bond stress for the GFRP #10 can be examined by experimental test data.

It should be cautioned that the bond stress distribution along the bar is increasingly non-linear, the longer the development length, and so the bond stress is only a reference value rather than a design property.

2.2.4 Adhesive-Bonded Anchors and Dowels Systems

According to Section 1.6.2 of FDOT Structures Design Guidelines [January 2020], the design tensile strength for adhesive anchor bond is calculated by:

$$\Phi N_c = \Phi_c \Psi_e \Psi_{gn} \Psi_m N_{bond} \tag{64}$$

Where:

$N_{bond} = \tau\pi d_b h_{ef} = 1.080 * 3.14 * 1.27 * 40 = 172.3\ k$

$A_{no} = (16d_b)^2 = 412.9$ (Figure 14)

$A_n = A_{gross} = 18^2 = 324$ (Figure 14)

$h_{ef} = l_d = 40$ in (Note: beyond 20d, this value is unconservative, per ACI 318-14)

$\Phi_c = 0.85$

$\Psi_e = 0.70 + 0.30$ (Cover / 8d) = 0.86

$\Psi_{gn} = A_n / A_{no} = 324 / 412.9 = 0.78$

$\Psi_m = 2.5 / (1 + z / h_{ef}) = 1$

τ= 1.08 ksi nominal bond strength for general use products on the APL (Type V and Type HV), however FDOT specifications require the use of Epoxy Compound Type AB, due to constructability reasons.

Design Commentary: It is advised by the FDOT Structures Design Office engineers that both the anchor group factor (Ψ_{gn}) and eccentricity modification factor (Ψ_m) are only applicable to concrete breakout failure modes and do not appreciably affect the adhesive bond resistance.

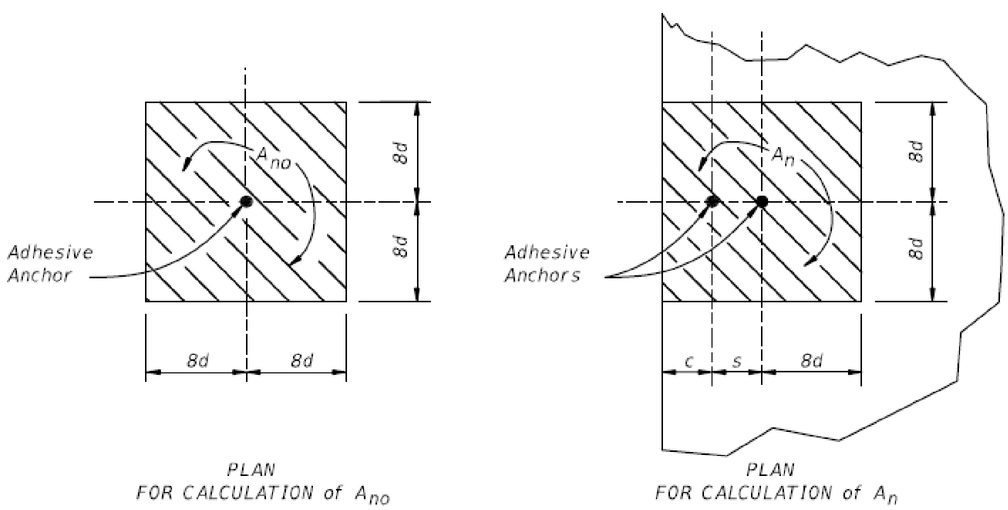

Figure 14: Effective tensile areas for adhesive anchors [FDOT Structures Design Guidelines January 2020]

After substitution to the Eq. 64:

$\Phi N_c = \Phi_c \Psi_e \Psi_{gn} \Psi_m N_{bond}$ = 0.85 ∗ 0.86 ∗ 0.78 ∗ 1 ∗ 172.3 = 98.2 k > 54.11 * 1.27 = 68.7 k

As a result, the design tensile strength for adhesive anchor bond is greater than the design tensile resistance of one GFRP bar, and therefore will allow the resistance to develop.

Again, it should be cautioned that the bond stress distribution along the adhesive dowel bar is increasingly non-linear, the longer the development length [Cook and Beresheim, 2002]. As such, ACI 318-14 (Chapter 17) advises that the linear bond stress model is not valid beyond 20 bar diameters. It is unknown whether this limit is applicable for GFRP dowel bars given that the tensile modulus of Elasticity is approximately on quarter of steel.

2.3 Development and Lap Splice Lengths for Conventional Steel (and Stainless Steel)

As indicated in the overall objectives and research approach, in this project, various combinations of material types for dowels and prestressing strands are to be evaluated. This includes conventional steel, stainless steel, and CFRP strands, and steel, stainless steel, CFRP and GFRP dowels. In this section, development and lap splice lengths for conventional steel is examined. These will be also applicable to the case of stainless steel strands and dowels.

ACI 318R-14 and AASHTO LRFD Bridge Design-8th Edition were used to calculate the development length and lap splice of steel dowels in pile splice.

2.3.1.1 ACI

Based on Section 25.4.2.3.9 of ACI 318R-14, for deformed steel bars or wires, the development length in tension shall be calculated by Eq. (65):

$$l_d = \left(\frac{3}{4d} \frac{f_y}{\lambda\sqrt{f'_c}} \frac{\psi_f \psi_e \psi_s}{\left(\frac{c_b + k_{tr}}{d_b}\right)} \right) d_b \tag{65}$$

In which, ψ_t, λ, ψ_e, ψ_s respectively are casting position, material, epoxy, and size factors which were calculated by:

$$\psi_t = 1 \text{ (Less than 12 in of fresh concrete placed below horizontal bar)} \quad (66)$$

$$\psi_e = 1 \text{ (No Epoxy coating on bar)} \quad (67)$$

$$\lambda = 1 \text{ (Normal weigth concrete)} \quad (68)$$

$$\psi_s = 1 \text{ (Bar size is larger than \#7)} \quad (69)$$

For the confinement term $\left(\frac{c_b+k_{tr}}{d_b}\right)$, k_{tr}, c_b, and d_b were calculated by:

$$k_{tr} = 40 * \frac{A_{tr}}{SR} = 40 * \frac{0.207^2 * \pi * \frac{1}{4}}{3*1} = 0.45 \quad (70)$$

$$c_b = 1.75 \text{ (Half of spacing)} \quad (71)$$

$$d_b = 1.27 \text{ (Diameter size for bar \#10)} \quad (72)$$

As a result, the development length for steel bar in tension, l_d, will be 42.65 in (1.08 m). The lap splice length of deformed bar in tension was calculated based on Section 25.5.2.1 of ACI 318-14. To develop yielding in the bars, $\frac{A_{s,provided}}{A_{s,required}} = 1$, and the splice type will be in the class B. Accordingly, using Eq. (73) the lap splice, l_{st}, is calculated to be 55.44" (1.4 m).

$$l_{st} = 1.3 * l_d = 1.3 * 42.65 = 55.44'' \quad (73)$$

2.3.1.2 AASHTO

Based on Section 5.10.8.2.1a-1 of AASHTO LRFD Bridge Design-8th Edition, for deformed steel bars, the development length in tension shall be calculated by:

$$l_d = l_{db}\left(\frac{\lambda_{rl} * \lambda_{cf} * \lambda_{rc} * \lambda_{er}}{\lambda}\right) \quad (74)$$

In which, ψ_t, λ, ψ_e, ψ_s respectively are casting position, material, epoxy, and size factors which were calculated by:

$$l_{db} = 2.4 d_b \frac{f_y}{\sqrt{f'_c}} = 74.7'' \quad (75)$$

$$\lambda_{rl} = 1 \text{ (Reinforcement location)} \quad (76)$$

$$\lambda_{cf} = 1 \text{ (Coating factor)} \quad (77)$$

$$\lambda_{rc} = \frac{d_b}{K_{tr}+C_b} = \frac{d_b}{(40\frac{A_{tr}}{Sn})+C_b} = \frac{1.27}{(40\frac{(\pi*0.207^2)/4}{3*1})+1.75} = 0.58 \text{ (Reinforcent confinement factor)} \quad (78)$$

$$\lambda_{er} = \frac{A_{s,required}}{A_{s,provided}} = 1 \text{ (Excess reinforcement factor)} \quad (79)$$

$$\lambda = 1 \ \text{(Concrete density modification factor)} \tag{80}$$

As a result, the development length for steel bar in tension, l_d, will be 43.2" in (1.09 m):

$$l_d = 74.7\left(\frac{1*2*0.58*1}{1}\right) = 43.2 \tag{81}$$

The lap splice for deformed bar in tension was also calculated based on Section 5.10.8.4.3A of AASHTO. The minimum length of lap splice in tension lap shall be as required for class A or B lap splice, but not less than 12 in. At the old version of AASHTO Specification, there was a Class C in which the lap splice calculated by $1.7l_d$, but at the new version of AASHTO, it is changed to Class B in which the splice length is $1.3l_d$. Therefore, the lap splice in tension is calculated to be 56.1 in (1.42m) by Eq. (82):

$$\text{lap splice} = 1.3 * l_d = 1.3 * 43.3 = 56.1'' \tag{82}$$

2.4 Resistance of Pile Splice using GFRP Dowel for Unforeseen Splice

It is realized that the case of unforeseen splices imposes some limitations on the length of holes that can be drilled into the lower segment of the piles. In communication with FDOT, it was determined that a practical drilling length is limited to 30 in. For the case of GFRP dowels however, this limitation does not affect the strength expected from the splice itself. As calculated in the previous sections, the development length of GFRP #10 bar in concrete is 25.4 in. Accordingly, the splice section in the unforeseen case will be able to develop the maximum nominal pure moment resistance of 206.1 k-ft (226.7 k-ft for proposed/improved properties). However, it is realized that the moment resistance in the lower segment of the pile immediately below the splice section may be limited by the limited lap splice of the GRFP bars with the prestressing strands. Nevertheless, this limitation will be present regardless of what type of dowel is used in the splice, and such, this limitation needs to be expressed clearly for the designer to consider. For the case of stainless steel strands, this will definitely limit the moment resistance for the lower segment of the pile. On the other hand, according to the calculation performed in this report, the development length for CFRP (CFCC) strand can be as low as 33.6 in., that is slightly bigger than the length of the hole to be drilled into the lower pile segment. Therefore, in the best scenario, when CFCC strand is used, the role of any auxiliary bar will be minimized. However, according to other sources, the development length of CFCC strand can be as high as 49 in. according to Mahmoud and Rizkalla, 1996, with Grace, 2000 α_t (Roddenberry et al. 2014). A consistent value for development length of CFCC cannot be established from the available literature, and experimental evaluation is needed to derive such. To allow the maximum attainable resistance for unforeseen splices, the length of holes to be drilled into the lower pile segment will be kept at its maximum practical length of 30 in., and the enhanced confinement provided by the tight spiral spacing at the head of the pile is anecdotally recognized.

2.5 M-N Interaction Diagrams for Pile and Splice

In the following sections, analyses are performed to compare the moment-axial force interaction results for piles using steel strands and splices using steel and GFRP material. Hand calculation using AASHTO and ACI codes, and layer-by-layer analysis using Response 2000 program are included.

2.5.1 Steel Strands and Dowels

For pile splice using conventional steel dowels, the results of hand calculations for moment axial force interaction diagram based on nominal strengths before application of resistance factor were compared to the results of Response 2000 in the same graph (Figure 15).

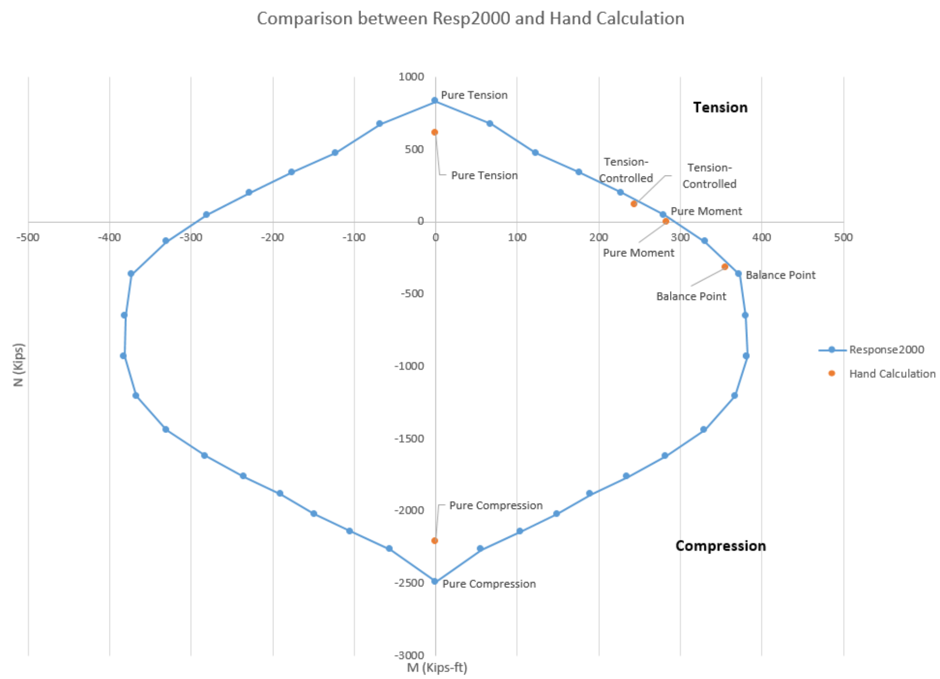

Figure 15: Comparison between results of hand calculation and Response 2000 for pile splice

As it is shown in Figure 15, the moment and axial force values obtained by hand calculation for three points of balanced, tension-controlled, and pure flexural match with the results calculated by Response 2000. However, for pure axial tensile and compressive strength, Response 2000 provides higher resistances. To make this comparison for design strengths, application of resistance factors are required. Table 11 shows resistance factors calculated based on ACI 318 R-14 and AASHTO LRFD Bridge Design-8th Edition.

Table 11: Resistance factors on AASHTO and ACI specifications

Resistance Factor	AASHT (Article 5.5.4.2.1)	ACI (Sec. 21.2)
Axial	0.75	0.65
Flexural	1.0	0.9

According to Table 11, the AASHTO resistance factors for pure tension, balanced condition, and pure compression were calculated to be 1.0, 0.75, and 0.75, respectively. The resistance factors at pure flexural point for pile and pile splice, respectively, were calculated to be 0.86 and 0.84 using a linear interpolation between two resistance factors of balanced and tension controlled points.

Similarly, the ACI resistance factors for pure tension, balanced condition, and pure compression were calculated to be 0.9, 0.65, and 0.65, respectively. The resistance factors at pure flexural point for pile and pile splice, respectively, were calculated to be 0.76 and 0.74 by using a linear interpolation between two resistance factors of balanced and tension controlled points. To check the calculated resistances for pile and splice against FDOT required resistances (Table 1), section analyses were carried out for a pile and pile splice using conventional steel strands utilizing Response 2000 (Figures 16 and 17).

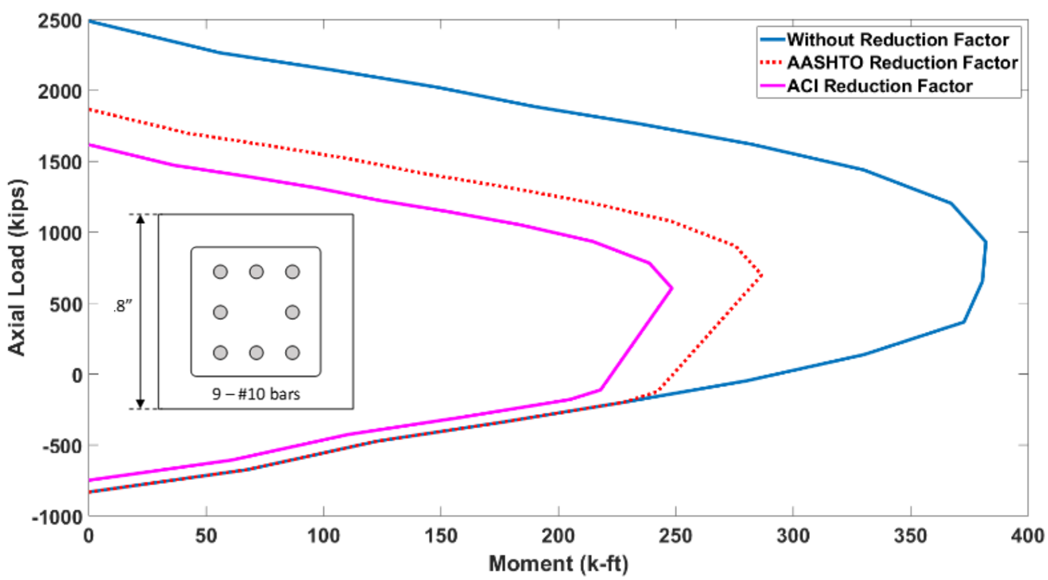

Figure 16: Comparison among M-N diagrams for pile splice using steel dowels

Figure 16 shows a comparison between the nominal and design moment-axial load interaction diagrams obtained using Response 2000 for pile splice with steel dowels in accordance with resistance factors from ACI 318 R-14 and AASHTO LRFD Bridge Design-8th Edition.

Interaction diagrams are shown in Figure 17 for an 18x18 in. pile for nominal and design strengths.

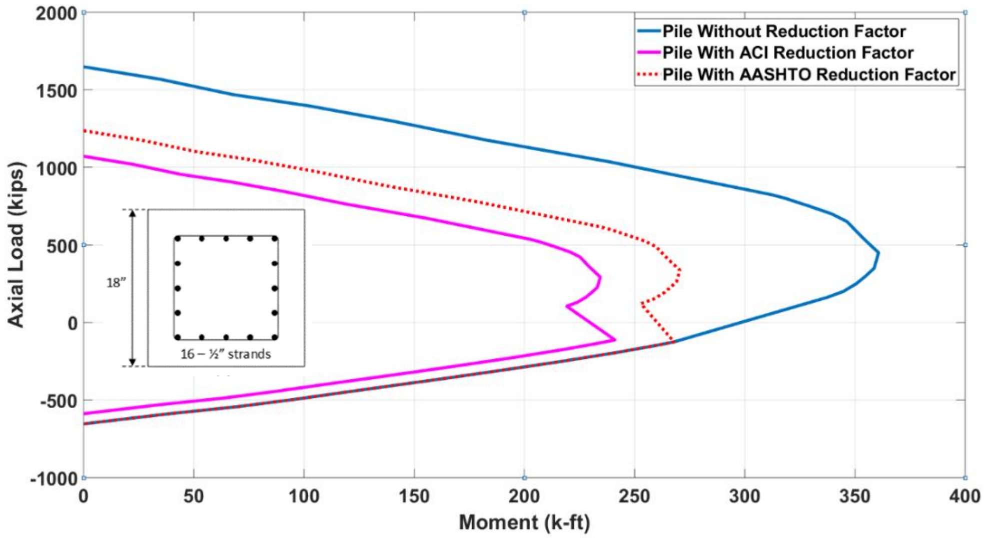

Figure 17: M-N diagrams for pile using steel strands

Table 12, summarizes the results for the pile and pile splice at pure axial compression, pure axial tension, pure flexural moment, and balanced points. At pure flexural moment, the results show that the pile splices provide resistance slightly smaller than the pile itself. Moreover, these results also show that a pile splice with 8-steel #10 steel dowels can develop 100% and 91% of the required design moment resistance (Table 1- 245 k-ft) when using the AASHTO and ACI resistance factors, respectively.

Table 12: Moment and force values for both pile and pile splice based on the different φ

Points	**without *φ*** Moment (k-ft), Force (kips)		**ACI *φ*** Moment (k-ft), Force (kips)		**AASHTO *φ*** Moment (k-ft), Force (kips)	
	Pile	Pile Splice	Pile	Pile Splice	Pile	Pile Splice
Pure Axial Compression	-- 0, 1616	-- 0, 2488	**0.65** 0, 1050	**0.65** 0, 1617	**0.75** 0, 1212	**0.75** 0, 1866
Balanced Failure	-- 360, 463	-- 382, 931	**0.65** 234, 301	**0.65** 248, 605	**0.75** 270, 347	**0.75** 286, 698
Pure Flexural Moment	-- 306, 0	-- 293, 0	**0.76** 233, 0	**0.74** 217, 0	**0.86** 263, 0	**0.84** 246, 0
Pure Axial Tension	-- 0, 660	-- 0, 831	**0.9** 0, 594	**0.9** 0, 748	**1** 0, 660	**1** 0, 831

Figure 18 provides a comparison between moment-axial force diagrams for pile and pile splice separately for nominal strengths and design strengths using AASHTO and ACI resistance factors.

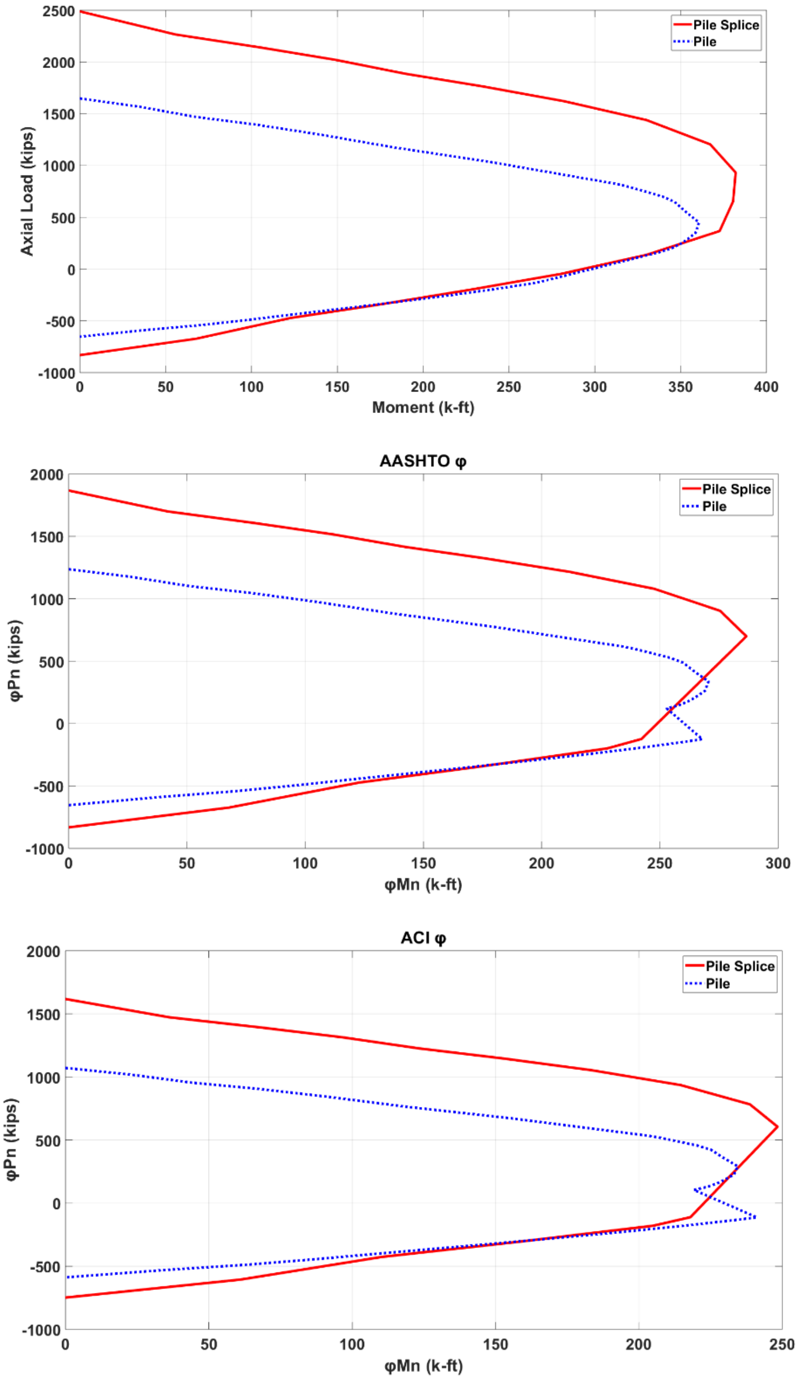

Figure 18: M-N interaction diagrams for pile and pile splice reinforced with conventional steel (Top: nominal strengths, middle: design using AASHTO , bottom: design using ACI φ)

2.5.2 Use of GFRP Dowels

Design moment-axial load interaction diagrams were calculated for pile splices using GFRP dowels of various size and configuration as discussed earlier. Hand calculations incorporated into Excel and MATLAB was employed to calculate and plot the M-N diagrams for these cases in Figure 19. Both current (2020) and proposed (2021) properties for GFRP dowels were considered.

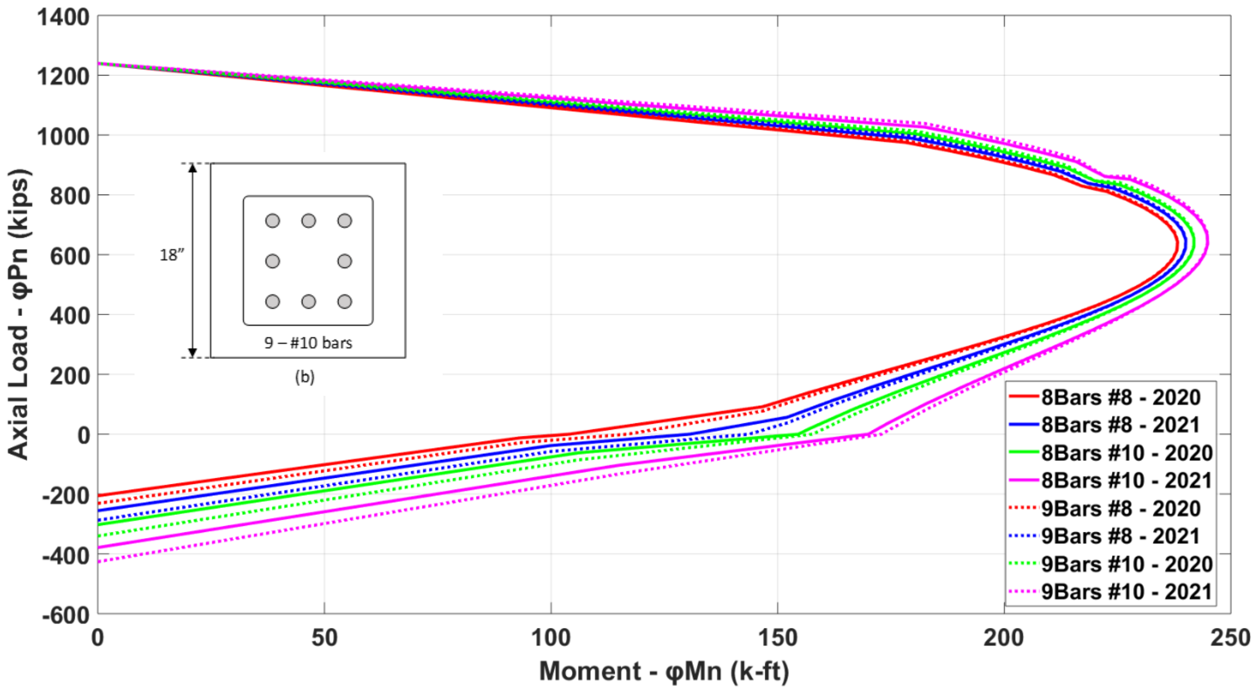

Figure 19: M-N interaction diagrams for all cases of the pile splice reinforced with GFRP

The comparison shows that using an additional dowel bar (9 vs. 8) in the splice has negligible effect in increasing the resistances. However, the use of improved GFRP dowel bar shows noticeable improvement in the resistances. The use of larger diameter dowel bars shows a significant improvement in the resistance.

2.5.3 Interaction Diagrams for Pile Splice using 8-# 10 GFRP and Steel Dowels

In this section, design moment-axial force interaction diagrams (based on AASHTO resistance factors) are compared for two cases of pile splice using 8-#10 steel and GFRP dowels (based on current GFRP properties). As it is shown in Figure 20, the pile splice using the GFRP dowels with 155 (k-ft) design moment resistance (at pure bending) can cover %63 of the design moment resistance of the steel pile splice using steel dowel with 246 (k-ft).

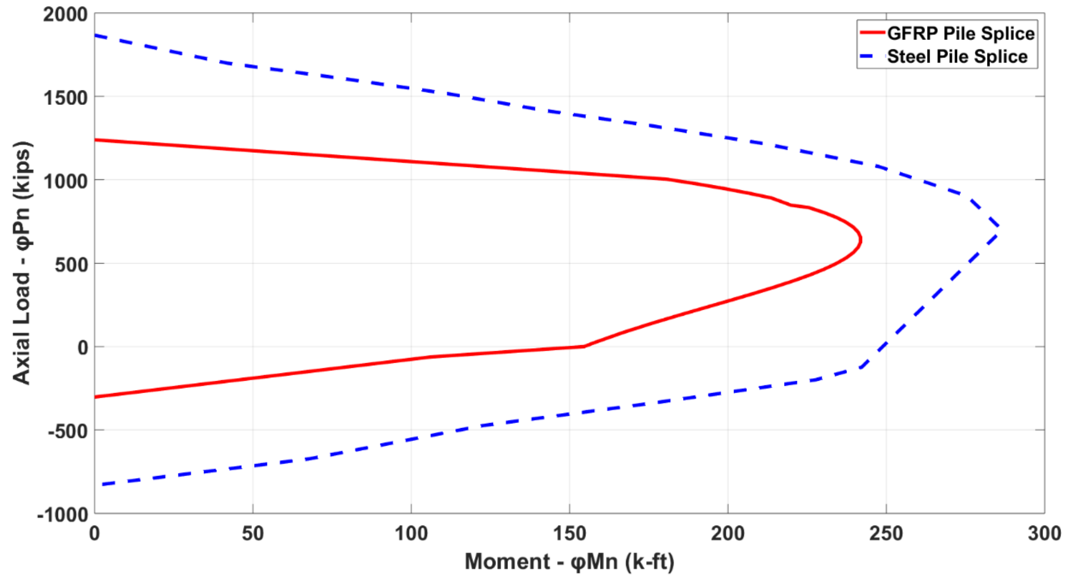

Figure 20: M-N interaction diagrams for pile splice reinforced with 8-bars #10 of steel and GFRP

2.5.4 Interaction Diagrams for Pile using 8-# 10 GFRP and Pile with Steel Strand

Design moment-axial force interaction diagrams (based on AASHTO resistance factors) are compared for a pile using steel strands and GFRP dowels (based on current GFRP properties). As it is shown in Figure 21, the pile splice with 155 (k-ft) design moment resistance (at pure bending) can cover %59 of pile design moment resistance with 263 (k-ft).

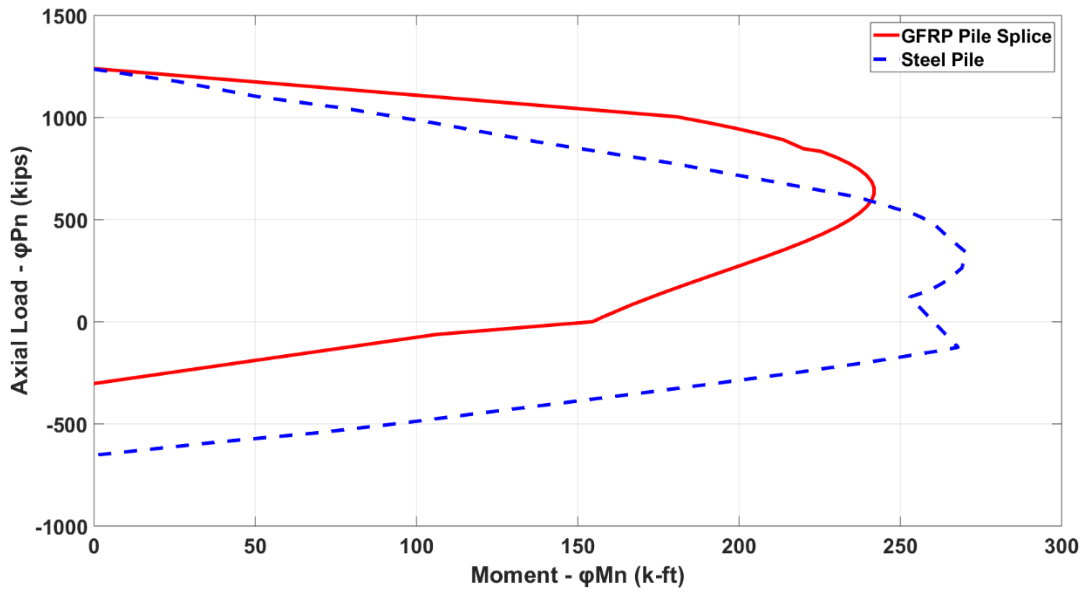

Figure 21: M-N interaction diagrams for pile splice reinforced with 8-bars #10 GFRP and steel strands pile

2.6 Proposed Design for Epoxy Dowel Splice using GFRP Bars

Based on the calculations for moment resistance and development and lap splice lengths presented above, Figures 22 and 23 shows the pile splice design with GFRP dowels with current properties.

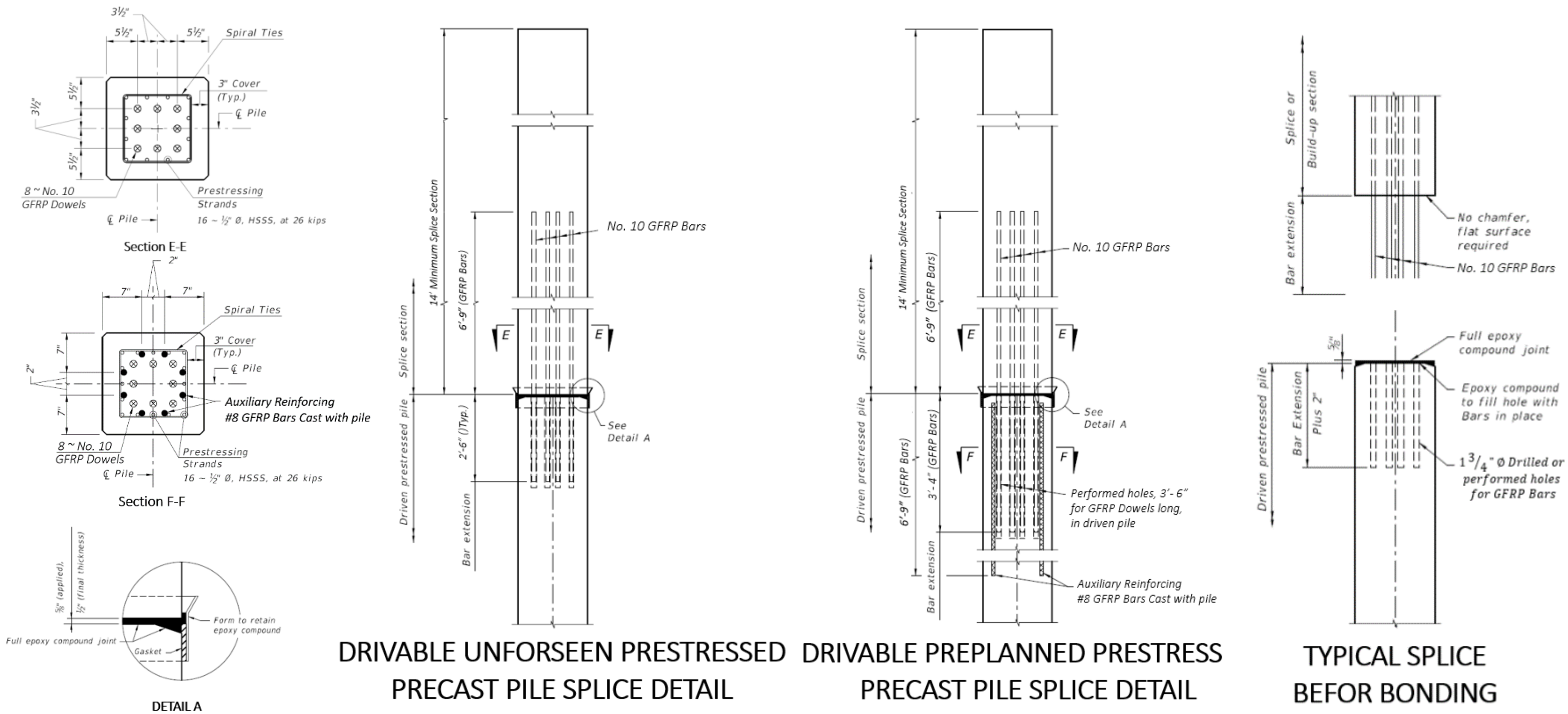

Figure 22: Development of Epoxy Dowel Pile Splice Design (SS Strands and GFRP Bars)

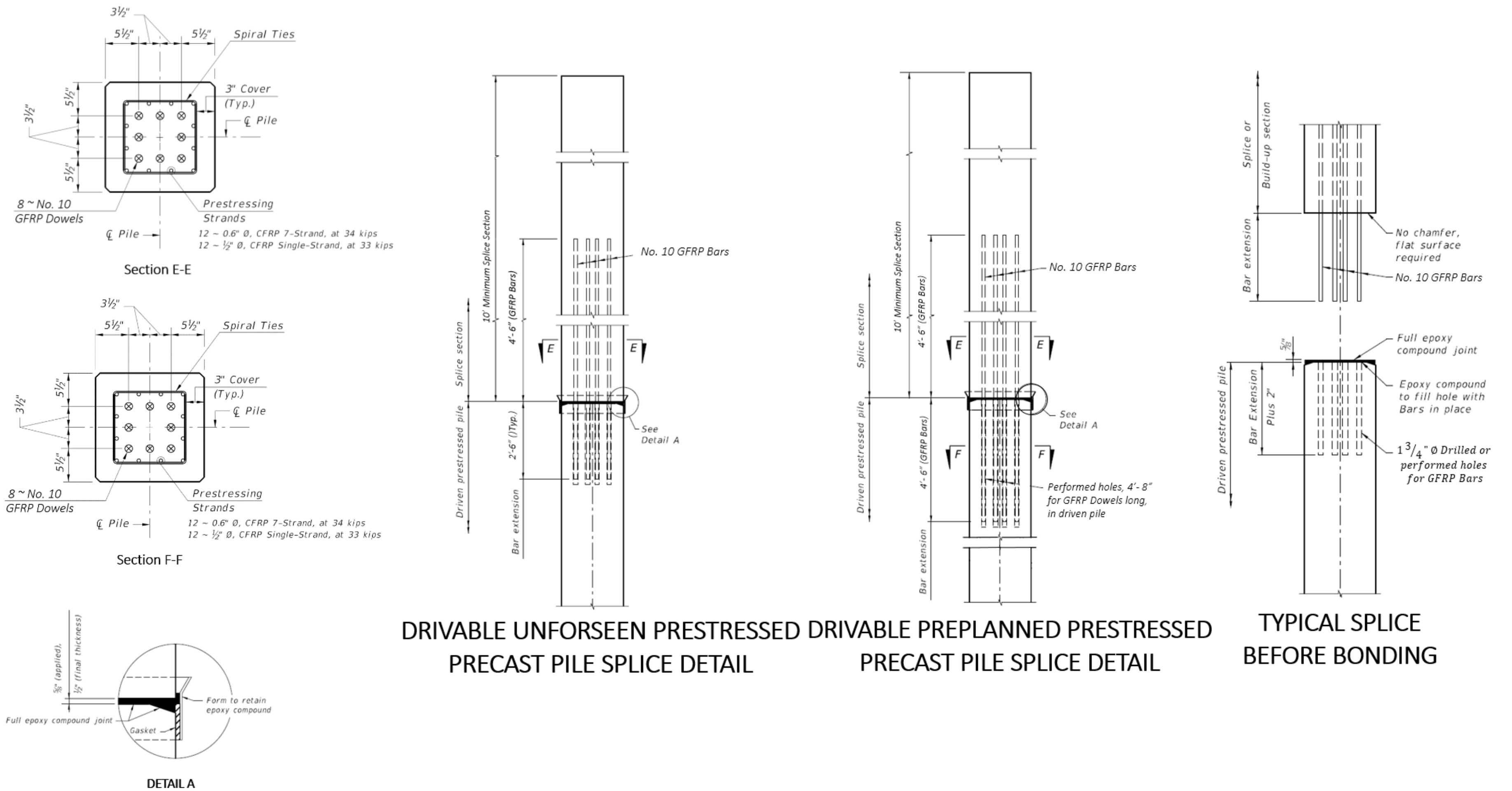

Figure 23: Development of Epoxy Dowel Pile Splice Design (CFRP Strands and GFRP Bars)

3 REFERENCES:

AASHTO (American Association of State Highway and Transportation Officials). 2017. AASHTO LRFD Bridge Design Specifications, 8th Edition, Washington, DC: AASHTO.

AASHTO (American Association of State Highway and Transportation Officials). 2018. AASHTO LRFD Bridge Design Specifications for GFRP-Reinforced Concrete, 2nd Edition, Washington, DC: AASHTO.

AASHTO (American Association of State Highway and Transportation Officials). 2018. AASHTO LRFD Bridge Design Guide Specifications for GFRP-Reinforced Concrete Bridges, 2nd Edition, Washington, DC: AASHTO.

AASHTO (American Association of State Highway and Transportation Officials). 2018. Guide Specifications for the Design of Concrete Bridge Beams Prestressed with Carbon Fiber-Reinforced Polymer (CFRP) Systems, 1st Edition, Washington, DC: AASHTO.ACI (American Concrete Institute) Committee 440. 2004. Prestressing Concrete Structures with FRP Tendons. ACI 440.4R-04. Farmington Hills, MI: ACI.

ACI (American Concrete Institute) Committee 440. 2004. Prestressing Concrete Structures with FRP Tendons. American Concrete Institute. ACI 440.4R-04.

ACI (American Concrete Institute) Committee 440. 2007. Report on Fiber Reinforced Polymer (FRP) Reinforcement for Concrete Structures. American Concrete Institute. ACI 440.R-07.

ACI Committee 318. 2014. Building Code Requirements for Structural Concrete (ACI 318-14) and Commentary (ACI 318R-14). Farmington Hills, MI: ACI.

ACI (American Concrete Institute) Committee 440. 2015. Guide for the Design and Construction of Concrete Reinforced with FRP Bars. American Concrete Institute. ACI 440.1R-15.

Cook, R.A. and Beresheim, S.D. (2002). “Post-Installed Adhesive-Bonded Splices in Bridge Decks.” (Report No. BC354 RPWO #2), University of Florida for Florida Dept. of Transportation.

FDOT Standard Plans s Index Series 455, (2021) Florida Department of Transportation, Tallahassee, FL.

Grace, N. (2000). “Transfer length of CFRP/CFCC strands for double-t girders.” PCI Journal, 45(5), 110–126.

Lu, Z., Boothby, T. E., Bakis, C. E., and Nanni, A. (2000). “Transfer and development length of FRP prestressing tendons.” PCI Journal, 45, 84–95.

Mahmoud, Z. I. and Rizkalla, S. H. (1996). “Bond properties of CFRP prestressing reinforcement.” Proceedings of the First Middle East Workshop on Structural Composites for Infrastructure Applications, Egypt.

Mullins, G., Sen, R., Sagüés, A., Winters, D., Morton, C., Fernandez, J., Johnson, K., DePianta, V., Vomacka, J. and Mitchell, E., 2014. Design and construction of precast piles with stainless reinforcing steel (Report No. BDK-84-977-07). Florida. Dept. of Transportation.

Paul, A., Kahn, L.F. and Kurtis, K., 2015. Corrosion-free precast prestressed concrete piles made with stainless steel reinforcement: construction, test and evaluation (No. FHWA-GA-15-1134). Georgia. Department of Transportation. Office of Research.

Standard Plans – Index Series 455. Florida Department of Transportation, Tallahassee, 2020-2021.

Standard Specifications for Road and Bridge Construction. Florida Department of Transportation, Tallahassee, January, 2020.

Structures Manual. Florida Department of Transportation, Tallahassee, January, 2021

Roddenberry, M., Mtenga, P. and Joshi, K., 2014. Investigation of carbon fiber composite cables (CFCC) in prestressed concrete piles (No. BDK83-977-17). Florida. Dept. of Transportation.

Technical Data on CFCC, 2012 Tokyo Rope.

Young, V., and Wan, G., "CFRP and HSSS Strands in Prestressed Concrete Design," FDOT Transportation Symposium, 2018.